



Analysis of ground response and potential seismic damage to sites surrounding Cimandiri Fault, West Java, Indonesia

Lindung Zalbuin Mase^{1,4}  · Andri Krisnandi Somantri² · Salisa Chaiyaput³ · Aditia Febriansya² · Arifan Jaya Syahbana⁴

Received: 11 May 2023 / Accepted: 22 August 2023 / Published online: 7 September 2023
© The Author(s), under exclusive licence to Springer Nature B.V. 2023

Abstract

Cimandiri Fault in West Java is one of the active faults in West Java, Indonesia. The activity of the fault could potentially result in damage to the surrounding areas. This paper presents a study of ground response analysis and the potential seismic damage to structures in sites surrounding the Cimandiri Fault. The site investigation data are collected. Furthermore, ground motion prediction is conducted. To estimate the potential damage, the potential seismic damage is performed. The spectral matching method determines artificial ground motion represented by the investigated sites. The seismic ground response analysis is conducted to observe ground motion parameters and soil response. The results show that the prediction of damage intensity level in the study area is about Scale VIII at maximum. The site amplification during seismic response is observed to vary from 1.4 to 2.7. The results also show that spectral acceleration design is still reliable in covering the effect of spectral acceleration amplification. However, the results also indicate that the trend of spectral acceleration shows that the amplification generally occurs at a medium-long period. It implies that the resonance effect may occur in medium-high-rise buildings.

Keywords Cimandiri fault · Ground response · Seismic damage · Site amplification

✉ Lindung Zalbuin Mase
lmase@unib.ac.id

¹ Department of Civil Engineering, Faculty of Engineering, University of Bengkulu, Bengkulu 38371, Indonesia

² Department of Civil Engineering, Bandung State Polytechnic, West Bandung, West Java 40559, Indonesia

³ Department of Civil Engineering, School of Engineering, King Mongkut's Institute of Technology Ladkrabang, Bangkok 10520, Thailand

⁴ Research Centre for Geological Disaster, National Research and Innovation Agency, Bandung 40135, Indonesia

1 Introduction

Indonesia is one of the countries in Southeast Asia that has frequently experienced many earthquakes (Paris et al. 2014). Within the last two decades, a sequence of earthquakes occurred in Indonesia. Several earthquakes, including the Aceh Earthquake in 2004, the Yogyakarta Earthquake in 2006, the Bengkulu-Mentawai Earthquake in 2007, the Padang Earthquake in 2009, and the Palu Earthquake in 2018 were known as devastating earthquakes that occurred in Indonesia. Hutchings and Mooney (2021) mentioned that Indonesian seismicity provides essential insights into the tectonics and hazards characterised by a remarkable diversity in faulting, including subduction, extension, thrusting, and strike-slip faulting. Those earthquakes were pieces of proof that the seismic intensity in Indonesia is extremely high.

West Java Province of Indonesia is one of the advanced provinces in Indonesia (Somantri et al. 2023). Several earthquakes occurred in this province, such as the M_w 7.7 Java Earthquake in 2006 and the M_w 6.8 Tasikmalaya Earthquake in 2009 (Mori et al. 2007; Bisri 2013). Those earthquakes are reported to result in significant damage in West Java Province. Muzli et al. (2021) suggested that those mentioned earthquakes occurred due to the activity of the Java Subduction Zone in the southern part of the province or Java Island (Fig. 1). Several researchers, such as Meilano et al. (2012); Supendi et al. (2018); Nugraha et al. (2019), mentioned that many active faults are located in West Java Province.

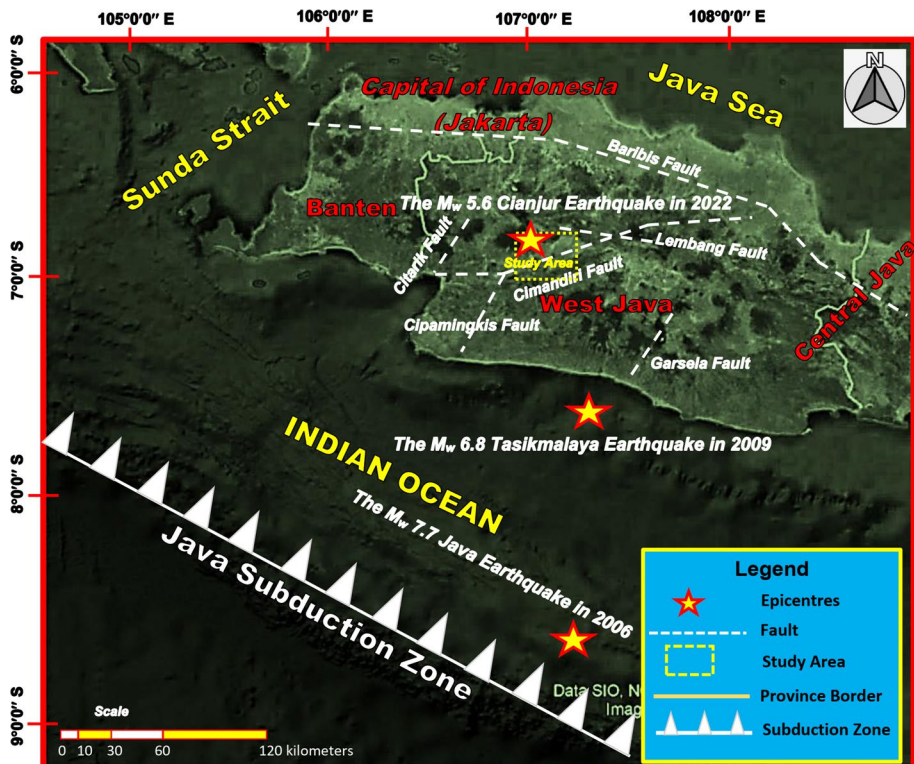


Fig. 1 Seismotectonic settings of West Java Province (modified from Somantri et al. 2023)

Lembang, Cimandiri, Baribis, Garsela, Cipamingkis and Citari Faults, are found in the West Java Province (Fig. 1). Somantri et al. (2023) predicted that Lembang Fault could result in significant seismic damage in Bandung Area, the capital city of West Java Province. In November 2022, an earthquake called the M_w 5.6 Cianjur Earthquake occurred in West Java Province and resulted in massive damage in the Cianjur Regency (Fig. 1). The earthquake is presumed to occur due to the activity of the Cimandiri Fault. This earthquake yielded about 600 death victims (National Agency for Disaster Countermeasures 2022). The earthquake is categorised as a slip-strike earthquake with a focal depth of about 11 km and a dip of 82.2° . The damage intensity level resulting from the earthquake is generally about Scale VII on Modified Mercalli Intensity (MMI) scale (Meteorological, Climatological, and Geophysical Agency 2022).

Cimandiri fault is one of West Java Province's active faults. This fault exists across many regencies and cities in West Java. According to Supendi et al. (2018), the slip rate of the Cimandiri fault is about 4 mm/year. Widiyantoro et al. (2022) mentioned that Cimandiri Fault could produce earthquakes with low to medium magnitude earthquakes. Marliyani et al. (2016) also suggested that Cimandiri Fault consisted of 6 segments: Loji, Cidadap, Nyalindung, Cibeber, Saguling and Padalarang. Gunawan and Widiyantoro (2019) also mentioned that the existence of the Cimandiri Fault in the south to the middle part of West Java could trigger a severe seismic hazard. Therefore, there is a need to study the possible impact in surrounding areas that could be affected by the fault. It is shown by how the shallow depth earthquake with a medium magnitude of M_w 5.6 could result in massive damage in the downtown area of Cianjur on November 21, 2022.

This paper presents the ground response analysis and the potential seismic damage to structures in sites surrounding the Cimandiri Fault, West Java, Indonesia. This study considers the recent earthquake event in this region, i.e. Indonesia's M_w 5.6 Cianjur Earthquake. Several sites investigation in Cimandiri Fault's surrounding areas were conducted. The prediction of ground motion is conducted. A spectral matching method to predict ground motion for the sites is conducted. Seismic ground response analysis is performed to observe ground response during the predicted earthquake. This paper discusses several fundamental findings, such as the prediction of damage intensity level, peak ground acceleration, and site amplification factor. This study also elaborates on the performance of the seismic design code against the seismic response. In general, this study could provide a better understanding of the possible impact of earthquakes resulting from the activity of the Cimandiri Fault.

2 Geological condition and seismic hazard risk

This study focused on West Java Province, especially on areas surrounding Cimandiri Fault. Figure 2 presents a geological map and layout of the site investigation conducted in this study. In Fig. 2, it can be observed that the study area has various and complex geological conditions. In addition, several faults are also captured in the study area. Several faults, such as Citarik Fault, Cipamingkis Fault, Cimandiri Fault, and Lembang Fault, surround the study area. The complex geological condition and various distributions of fault indicate that the area is categorised as an active tectonic setting region. Also, seven sites are investigated in this study. Detailed information related to the coordinates of each site is presented in Table 1. Cimandiri Fault is categorised as a slip-strike fault with a length of 100 km and is covered by recent volcanic products (Febriani 2016). The investigated sites include

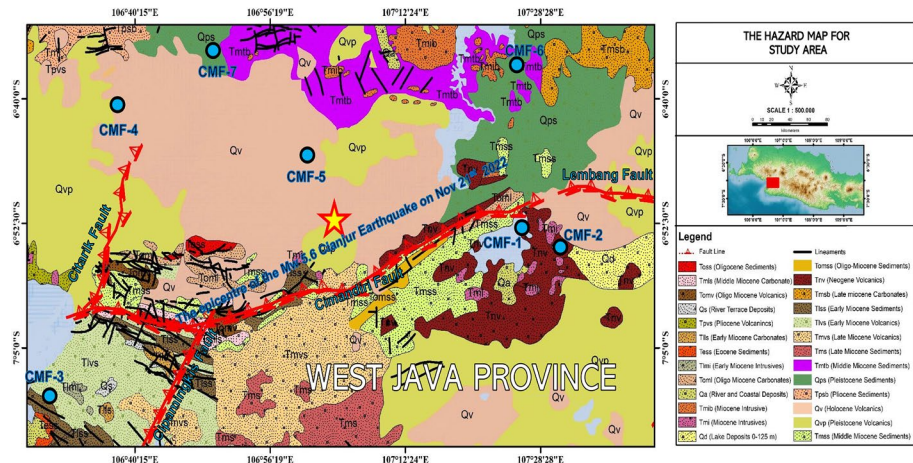


Fig. 2 The geological map and the layout of the site investigation (modified from the Geological Research and Development Centre 2023)

Table 1 The coordinates and locations of the site investigations in the study area

Sites	City	Latitude (°)	Longitude (°)	V _{s30} (m/s)	Focal depth (km)
CMF-1	Parahyangan	6° 52' 04.12" S	107° 27' 16.45" E	221.52	–
CMF-2	Cimahi	6° 54' 12.74" S	107° 32' 04.95" E	252.51	–
CMF-3	Ciletuh	7° 10' 50.09" S	106° 27' 56.22" E	310.97	–
CMF-4	Sukabumi	6° 36' 43.85" S	106° 37' 18.57" E	190.64	–
CMF-5	Cianjur	6° 43' 00.38" S	107° 00' 40.05" E	244.29	–
CMF-6	Purwakarta	6° 32' 55.64" S	107° 26' 45.98" E	238.44	–
CMF-7	Cibinong	6° 30' 08.56" S	106° 49' 38.87" E	256.13	–
Epicentre	Cianjur	6° 51' 10.80" S	107° 05' 42.00" E	–	11

seven cities surrounding the Cimandiri Fault. They are noted as CMF-1 to CMF-7. CMF-1 is in Parahyangan, CMF-2 is in Cimahi, CMF-3 is in Ciletuh, CMF-4 is in Sukabumi, and CMF-5 is in Cianjur, CMF-6 is located in Purwakarta, and CMF-7 is located in Cibinong. All cities are located in West Java Province and are categorised as important areas to support West Java Province’s social and economic development. Figure 2 shows the position of the earthquake’s epicentre. All cities are also within a 70 km radius of the earthquake epicentre. The earthquake is categorised as a shallow crustal earthquake.

In line with Fig. 2, active tectonic settings in the study area are certainly putting the study area very vulnerable to undergoing earthquake damage. Figure 3 presents the seismic hazard map in the study area with a return period of 2500 years and a 2% probability of exceedance within 50 years. In Fig. 3, it can be observed that there are five zones of peak ground acceleration or PGA in the study area. PGA, with the range of 0.5–0.6 g, is the first dominant PGA in the study area. CMF-7, CMF-5, CMF-1, and CMF-2 fall into this zone. CMF-6 in the northern part of the study area tends to have PGA ranging from 0.4 to

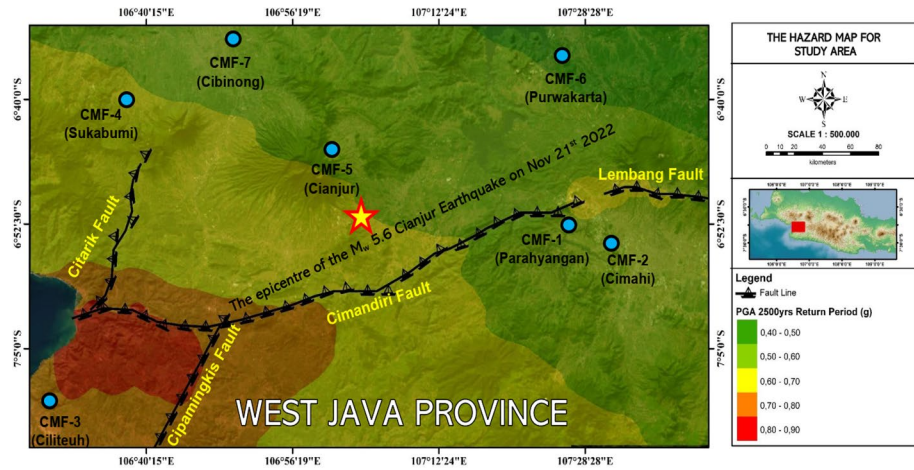


Fig. 3 Seismic hazard map of the study area

0.5 g. CMF-5 falls into the PGA zone ranging from 0.6 to 0.7 g, whereas CMF-3 falls into the PGA zone ranging from 0.7 to 0.8 g. According to SNI 1726:2019 (2019), PGA ranging from 0.17 to 0.57 g and PGA more than 0.57 g are categorised as moderate to strong motion. In general, the level of seismic hazard is categorised as high, in which the study area could undergo moderate to strong motion effects.

At those locations (CMF-1 to CMF-7), site investigations are conducted. Site investigations are boring log-standard penetration tests (SPT) and shear wave velocity measurements. The results of the site investigation are presented in Fig. 4. In Fig. 4, it can be observed that clayey soils and sandy soils are dominant in the study area. Several types of clayey soils, such as organic clay (OL), high-plasticity clay (CH), and low-plasticity clay (CL). These soil types tend to have a thickness variation of about 1–10 m. Silty soils, such as low-plasticity silt (ML) and high-plasticity silt (MH), are also found in the investigated areas. The thickness of silty soils in the investigated sites is observed to vary from 2 to 10 m. For granular soils, sands classified as clayey sand (SC), silty sand (SM), poorly graded sand (SP), and well-graded sand (SW) are found. These sand layers tend to have thickness observed to vary from 1 to 10 m. In addition, well-graded gravel (GW) is also found, with a thickness of about 10 m.

In terms of soil resistance, it can be observed that several sites, such as CMF-2, CMF-4, and CMF-6, tend to reach the stiff layers (indicated by (N-SPT of 60 blows/ft) at shallow depth. The depth of the stiff layer in these sites is observed to vary from 20 to 25 m. For CMF-5 and CMF-7, the stiff layer is found at a depth of 30 m. For CMF-1 and CMF-3, the depth of the stiff layer is generally found at 40 m. Therefore, based on the site investigation, it can be estimated that the depth of the stiff layer is observed to vary from 20 to 40 m. In terms of time-averaged shear wave velocity for the first 30 m depth (V_{s30}), it can be observed that V_{s30} in the investigated sites is observed to vary from 190 to 311 m/s. According to National Earthquake Hazard Reduction Program or NEHRP (1998), Sites having V_{s30} within the range of 180–360 m/s are categorised as Stiff Soils Sites or Site Class D. Based on studies conducted by Dolce et al. (2003), Mase et al. (2021a), and Ade-movic et al. (2022), Sites categorised as Site Class D could be vulnerable to undergo seismic impact during an earthquake. Since the site investigated areas are categorised as Site

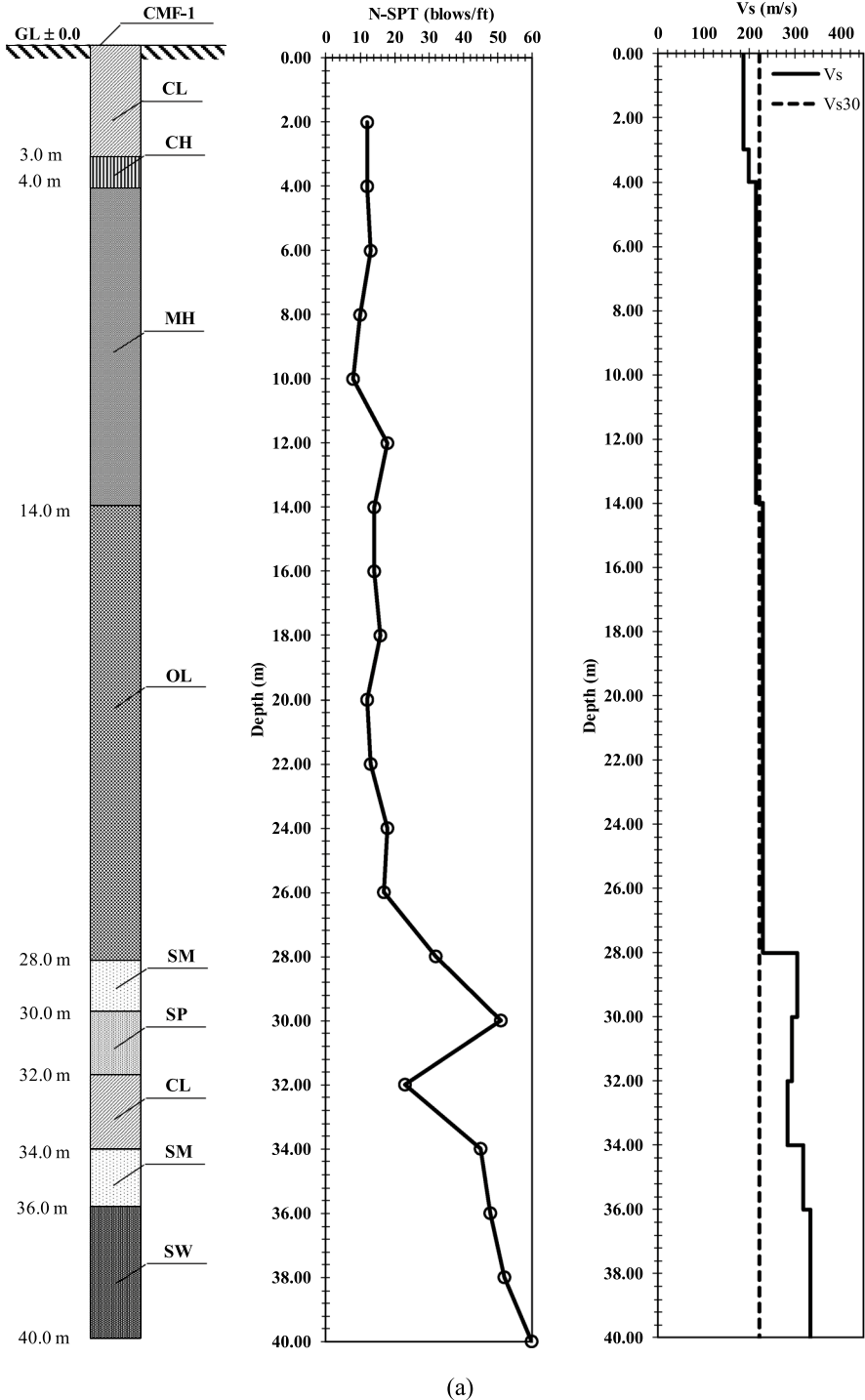
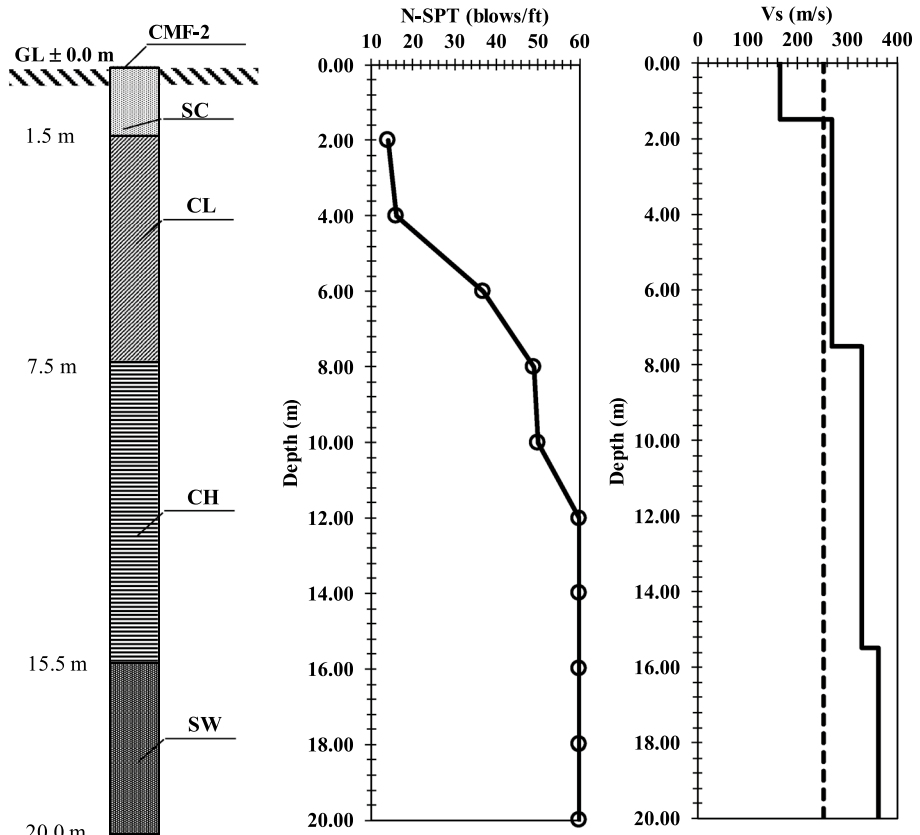


Fig. 4 Site investigation results in a CMF-1, b CMF-2, c CMF-3, d CMF-4, e CMF-5, f CMF-6, g CMF-7



(b)

Fig. 4 (continued)

Class D; therefore, it is essential to observe the potential seismic damage to the structure in the study area.

3 Theory and method

3.1 Ground motion prediction, spectral matching method and artificial ground motion

An essential factor, i.e. ground motion, should be defined to observe ground response and the potential seismic damage to the structures. In practical engineering, the ground response effect could be used to estimate potential seismic damage, amplification and other potential damage, such as liquefaction and landslides. This study’s primary goal is to perform seismic ground response analysis, but the ground motion record in the observed sites has yet to be available. The Cimandiri Fault is the active tectonic region in West Java Province. Since the earthquake mechanism under Cimandiri Fault is categorised as a shallow

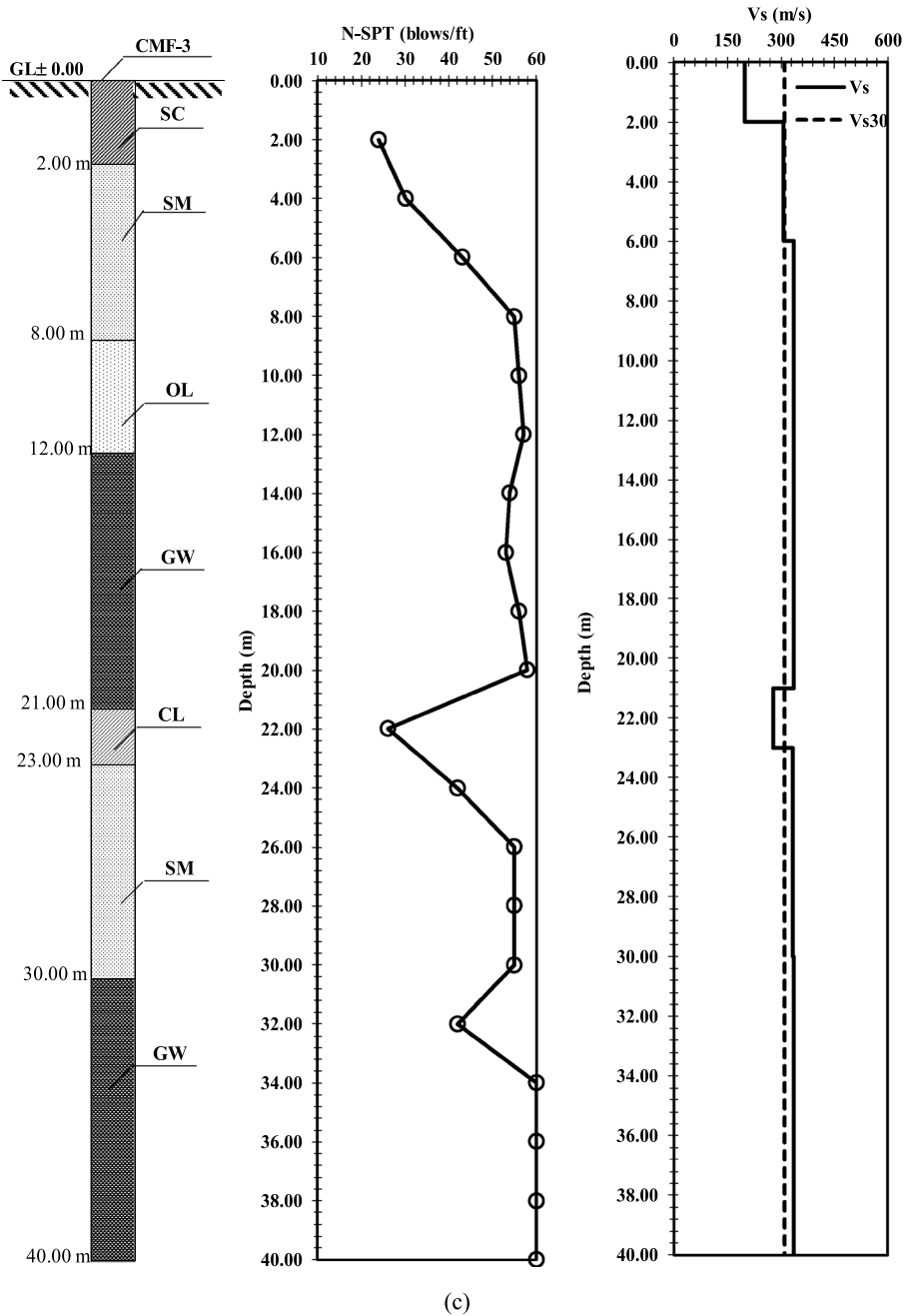


Fig. 4 (continued)

crustal earthquake, the attenuation models used for ground motion prediction should also be attenuation models for shallow crustal earthquakes. In this study, ground motion prediction is conducted based on attenuation models called “Next Generation Attenuation West2

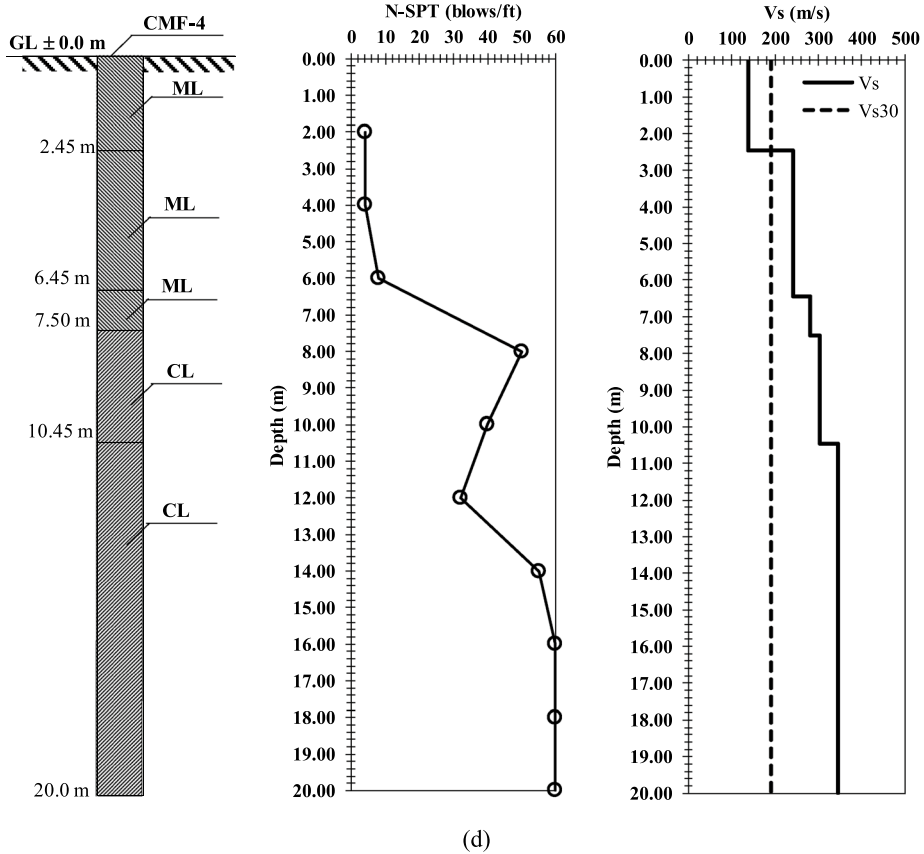


Fig. 4 (continued)

or NGA-West2 models (Bozorgnia et al. 2014). Since the investigated sites are within a radius of 200 km from the epicentre of the M_w 5.6 Cianjur Earthquake in 2022, NGA-West2 is still applicable to implement (Tanapalungkorn et al. 2020). The models include Abrahamson et al. (2014), Boore et al. (2014), Campbell and Bozorgnia (2014), Chiou and Youngs (2014), and Idriss (2014). Those models are addressed to predict spectral and peak ground acceleration in the study area categorised as soil and rock sites. It should be noted that Idriss’ (2014) model applies to rock sites, whereas other models apply to soil sites. Seyhan (2014) and Gülerce et al. (2017) suggested that the weighted average of NGA-West2 models should be implemented to minimise the uncertainty effect that could influence the variation of ground motion.

From NGA-West2 models, spectral accelerations are generated. From the spectral acceleration, peak ground acceleration can be estimated as spectral acceleration at 0 s. As mentioned in the previous explanation, there are no ground motion records for each investigated site. Therefore, the spectral matching method from Hancock et al. (2006) can be implemented to generate the input motion for the investigated sites. Mase et al. (2022a) and Somantri et al. (2023) suggested that the spectral matching method could be applicable considering the uncertainty of sites and ground motion. This study uses some ground

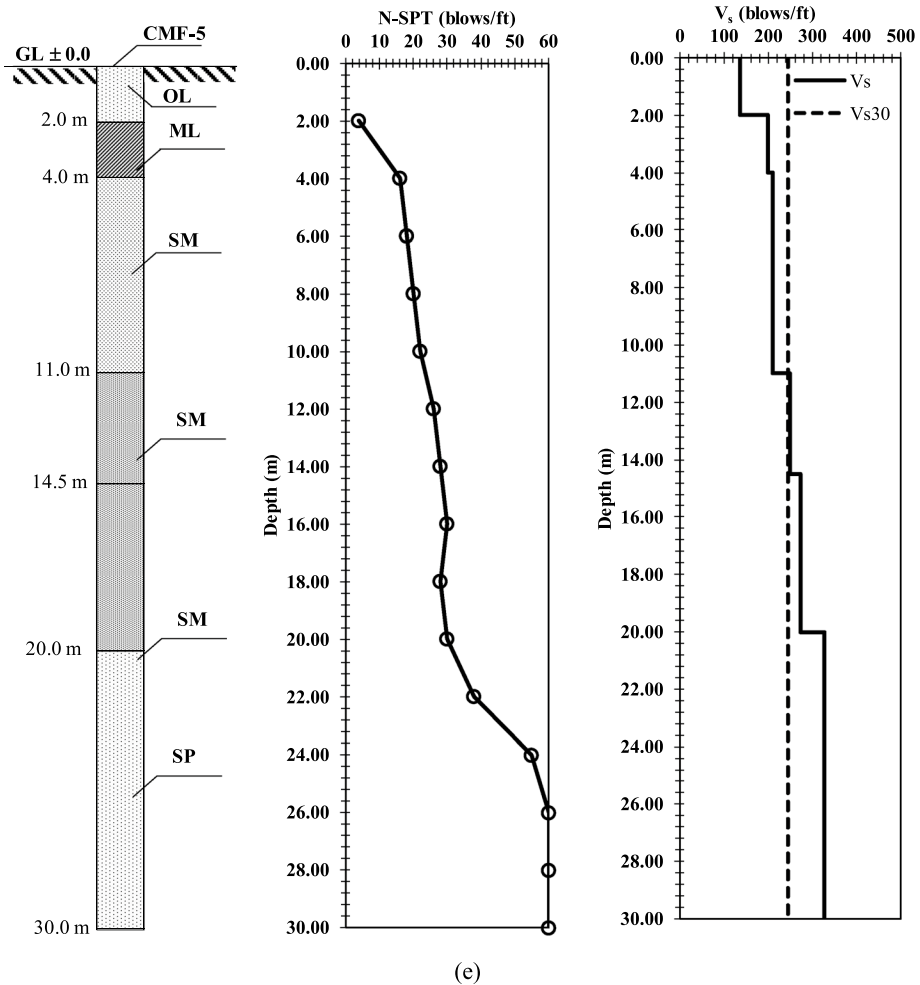
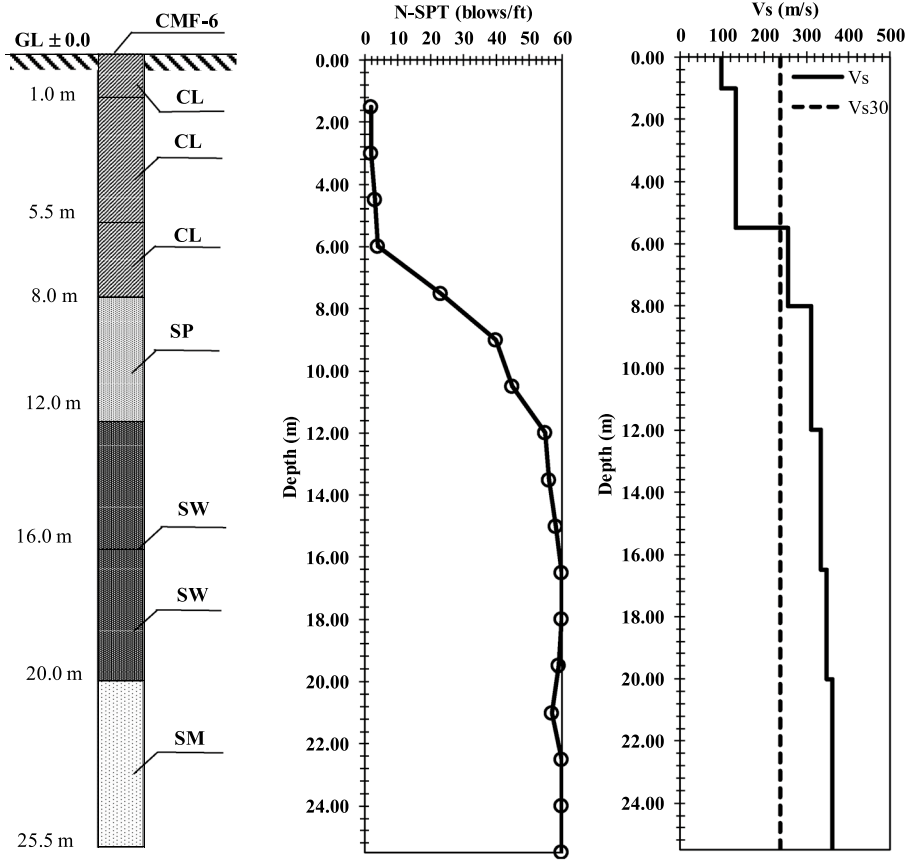


Fig. 4 (continued)

motion records from historical earthquakes under the exact earthquake mechanism as the Cianjur Earthquake in 2022. The ground motions from the Kobe Earthquake in 1995, the Loma Prieta Earthquake in 1989, the Friuli Earthquake in 1976, Imperial Valley Earthquake in 1973 and Northridge Earthquake in 1994 are used. Mase (2018) also suggested that the minimum five ground motions could be applicable for seismic analysis purposes. The process emphasises the matching of spectral acceleration between recorded ground motion and the prediction. The predicted spectral acceleration from NGA-West2 is assumed as the target spectral acceleration. The target spectral acceleration should represent several parameters influencing the ground motion, such as earthquake magnitude, site condition, distance to the rupture, and earthquake mechanism (Mase et al. 2022a). In NGA-West2, those uncertainty parameters have been considered. The process is conducted iteratively until the matching spectral acceleration is consistent with the target spectral acceleration. The matched spectral acceleration is then back-analysed to the defined site-ground motion.



(f)

Fig. 4 (continued)

3.2 One-dimensional seismic ground response analysis

One-dimensional seismic ground response analysis is performed to observe the ground response during seismic wave propagation. A nonlinear model for ground response analysis is generally used because this model is relatively appropriate to model the nonlinear behaviour of soil during an earthquake (Adampira et al. 2015). Misliniyati et al. (2019) analysed the applicability of soil models for one-dimensional seismic ground response analysis. They concluded that a nonlinear model, especially pressure dependent hyperbolic from Hashash et al. (2020), is generally reasonable for predicting ground motion during a strong earthquake. Several studies conducted by Likitlersuang et al. (2020), Qodri et al. (2021), and Bessette and Yniesta (2023) confirmed that the use of a pressure-dependent hyperbolic model is successfully implemented to predict ground response and soil behaviour during an earthquake.

This study employs the pressure-dependent hyperbolic model from Hashash et al. (2020) to observe ground response during seismic excitation for sites surrounding the Cianjur Earthquake in 2022. The model was initially developed by Matasovic (1993) and extended

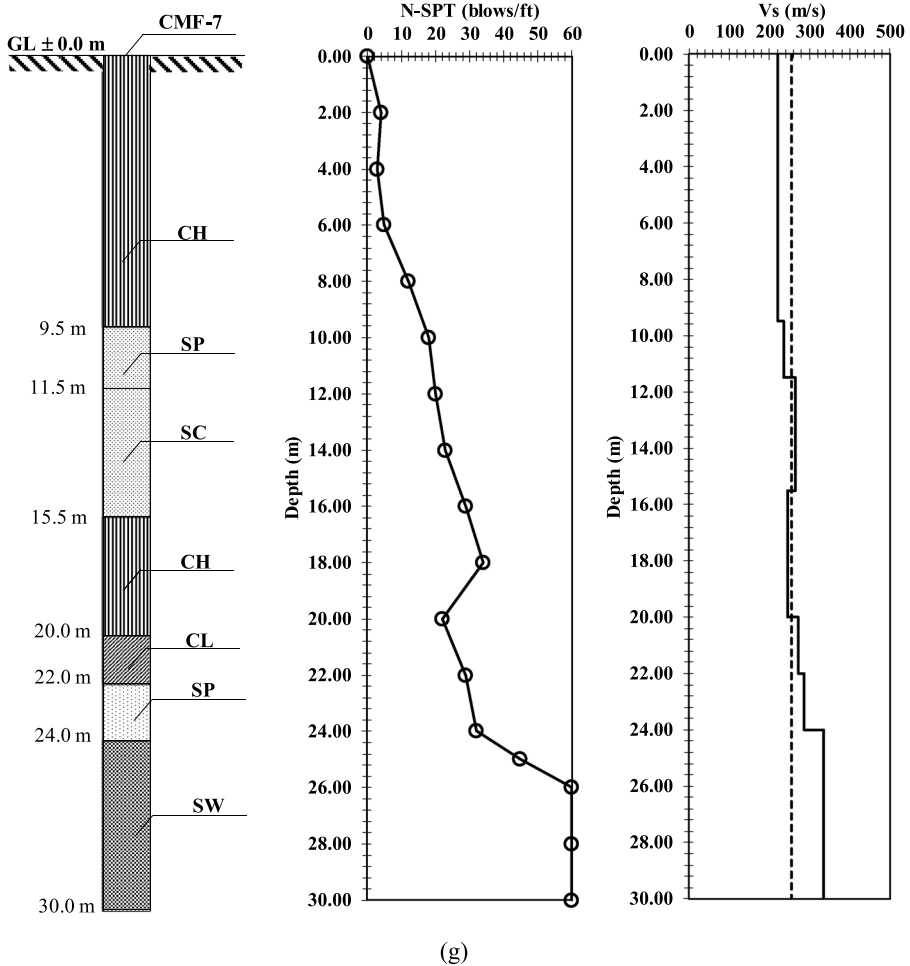


Fig. 4 (continued)

by Hashash and Park (2001). Mase et al. (2022b) suggested that the model emphasises the hysteretic loop during cyclic loading. The model defines the backbone curve for the hysteresis loop based on the hyperbolic function, which was first developed by Dunchan and Chang (1970). The mass-lumped system is the analysis framework implemented in the model by Hashash et al. (2020). It analyses ground response by applying input motion at the bottom of investigated sites. This study did not perform a dynamic experiment to determine the shear modulus reduction curve ($G/G_{\max} - \gamma$). Therefore, to overcome this limitation, shear modulus reduction curves from the study of Somantri et al. (2023) are implemented in this study (Fig. 5). Since the study is close to the study area of Somantri et al. (2023), i.e. Bandung Region, which is also in West Java Province, the use of the curves is reasonable for engineering practice. Hashash et al. (2020) suggested minimising the high-frequency effect in the analysis regarding horizontally-layered soils. The determination of layer thickness in the analysis should be considered. Equation 1 expresses the formulation to determine sub-layer thickness in the analysis as follows,

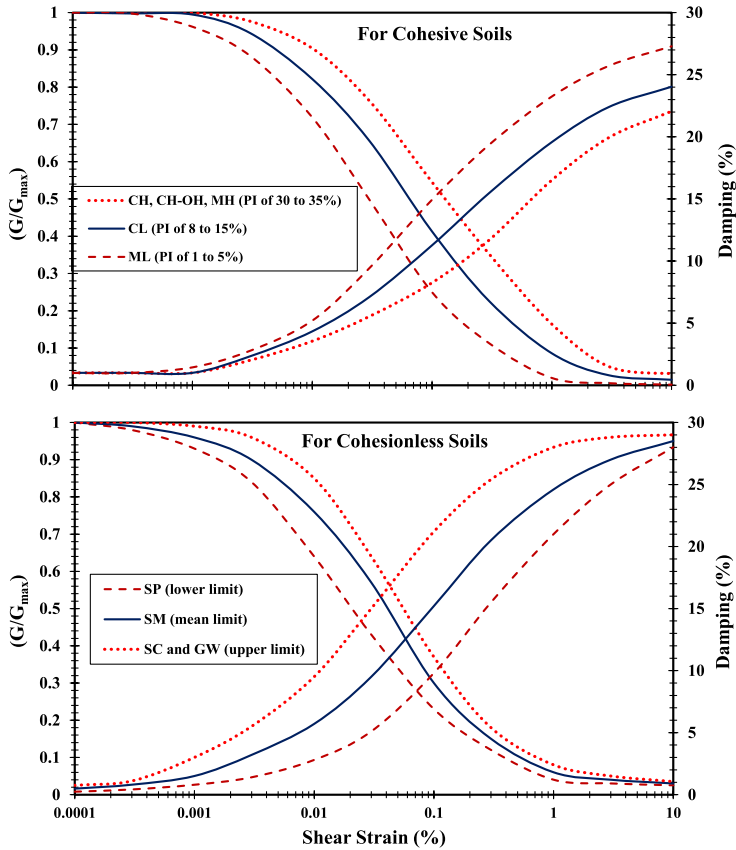


Fig. 5 Shear modulus reduction curve (modified from Somantri et al. 2023)

$$d = \frac{V_s}{4f_{\max}} \tag{1}$$

where d is the sub-layer thickness, V_s is the shear wave velocity of the layer, and f is the maximum frequency. Hashash et al. (2020) recommended that layers have the same maximum frequency throughout the soil profile. A f_{\max} should generally be at a minimum of 30 Hz.

The input motion is applied at the bottom of each site investigation, in which the bottom of the soil profile is assumed as an elastic half-space, and there is no drainage through the bottom boundary. Mase et al. (2022c) and Somantri et al. (2023) suggested that engineering bedrock for elastic half-space could be assigned for the layer having V_s ranging from 300 to 700 m/s. During seismic wave propagation, the ground response results are presented, including the peak ground acceleration (PGA) profile, acceleration time history, spectral acceleration, and amplification. For amplification factor, it is estimated by using the following equation,

$$AF = \frac{PGA_{\max(\text{at surface})}}{PGA_{\max(\text{input motion})}} \quad (2)$$

where AF is the amplification factor, $PGA_{\max(\text{at the surface})}$ is peak ground acceleration at the ground surface, and $PGA_{\max(\text{input motion})}$ is peak ground acceleration of the input motion.

The results of seismic ground response analysis, especially PGA at the surface, could be used for further analysis to estimate damage intensity levels. Tjockrodimuljo (2000) mentioned a relationship between Modified Mercalli Intensity and the PGA. Tjockrodimuljo (2000) and Mase (2020) suggested that Modified Mercalli Intensity could be significant in describing the earthquake's destruction. For the Modified Mercalli Intensity (MMI) level to predict the level of seismic damage to the structure, the following equation is implemented,

$$\log(\text{PGA}) = \left(\frac{1}{4}\text{MMI}\right) + \frac{1}{4} \quad (3)$$

PGA is peak ground acceleration (in gal) and MMI is the damage intensity level.

3.3 Research framework

The research framework implemented in this study is presented in Fig. 6. This work is started by investigating site areas surrounding the Cimandiri Fault. Several pieces of information, such as the characteristic of the Cimandiri Fault and the earthquake history in West Java, are also collected. Furthermore, ground motion prediction using next-generation attenuation (NGA) models is also performed. This analysis also obtained site spectral acceleration considered weighted factor and uncertainty.

The spectral matching method is implemented to generate the input motion for the investigated sites. Five ground motions from different sources are used to reduce the uncertainty effect. The spectral matching method generates the artificial ground motion based on the minimum misfit for the matched spectral acceleration for each site. Afterwards, the one-dimensional seismic ground response analysis is conducted.

In this study, a pressure-dependent hyperbolic model in the framework of the mass-lumped system is employed to observe ground response during seismic wave propagation. The assumption of engineering bedrock at the bottom of the soil profile is also adopted based on previous studies conducted in similar areas' characteristics. Several results, such as maximum acceleration profiles, the time history of acceleration, site amplification factor (AF), and prediction of MMI level, are also presented. Spectral acceleration comparison based on ground response analysis is also made to inspect the reliability of the actual seismic design code in the study area. The discussion on the relationship between MMI, V_{s30} , and distance to surface projection (R_{jb}) is also presented in this study.

4 Results and discussion

4.1 Ground motion prediction and the input motion for sites

Figure 7 presents the results of the NGA model analysis for each investigated site. In Fig. 7, sites' spectral accelerations include three main curves. The first is the median curve, and the other two are the upper and lower boundary curves. Based on the analysis, peak ground

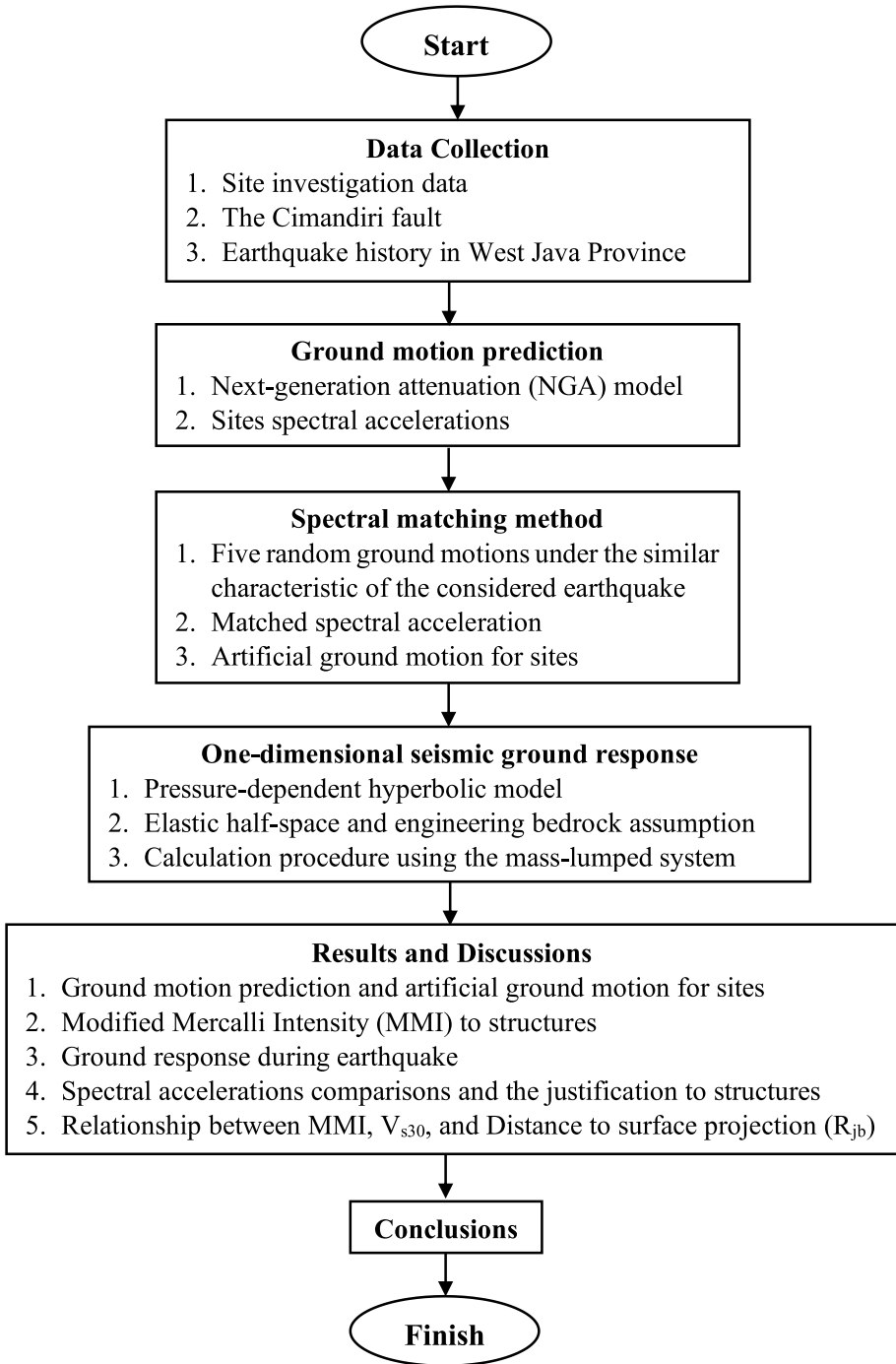


Fig. 6 Research framework

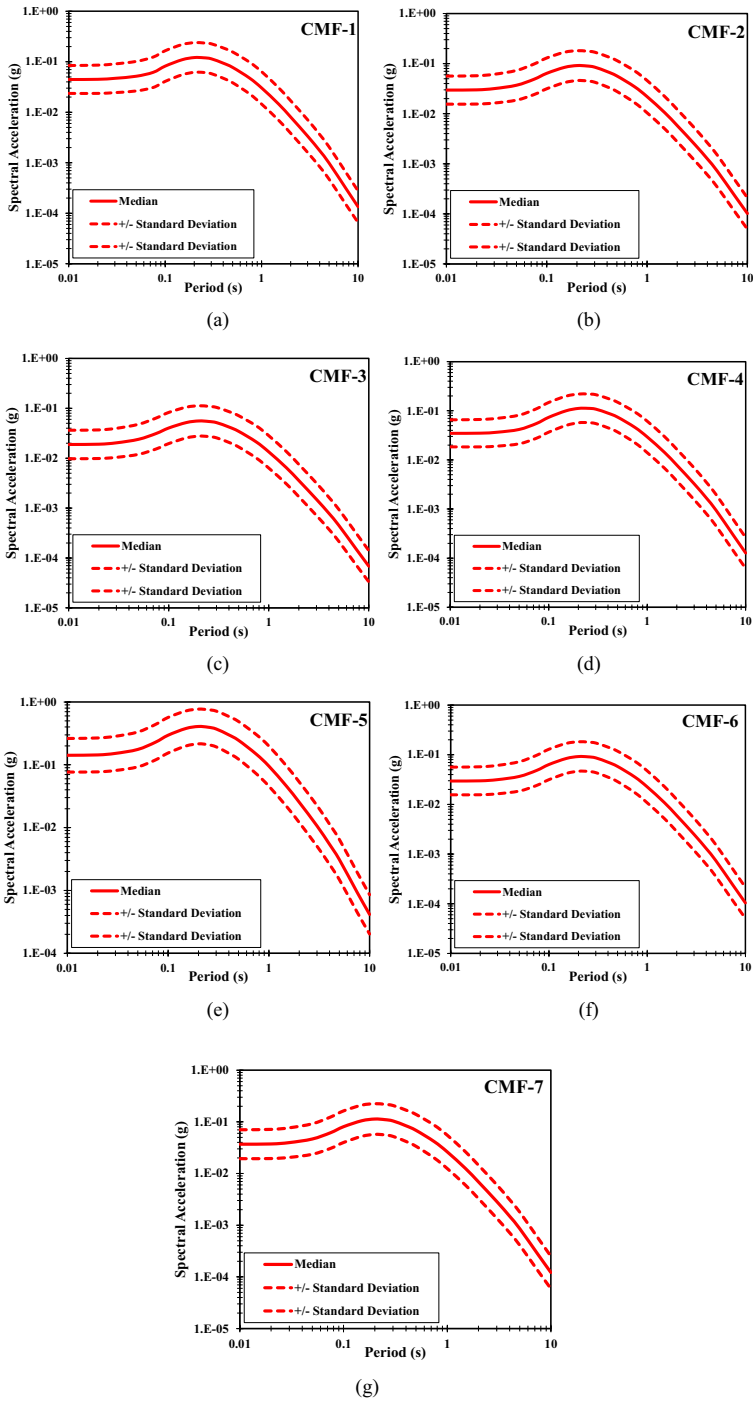


Fig. 7 Spectral accelerations of sites based on NGA models for **a** CMF-1, **b** CMF-2, **c** CMF-3, **d** CMF-4, **e** CMF-5, **f** CMF-6, **g** CMF-7

acceleration (PGA) in the investigated sites is observed to vary from 0.023 to 0.135 g. the maximum PGA value is found in CMF-5, whereas the minimum is in CMF-3. CMF-3 is the farthest site, and CMF-5 is the closest to the epicentre. Therefore, it seems reasonable why the closest site tends to have the maximum PGA value. Based on the United States Geological Survey or USGS, the maximum PGA during an earthquake is about 0.145 g. Figure 7 also presents that spectral acceleration for CMF-5 is generally higher than spectral acceleration compared to other spectral acceleration in other investigated sites. This is because the position of CMF-5 is very close to the earthquake epicentre. Therefore, the spectral response could be more significant than other sites located further than the epicentre.

As explained in the previous section, five ground motions from different sources are used to match spectral accelerations. Table 2 summarises the spectral matching results for ground motion selection. To make justification in selecting the representative ground motions. The average misfit from the spectral matching method is used. The red colour fonts in Table 2 indicate the best-matched ground motion on each site. The Kobe motion is reliable for scaled motions for CMF-1, CMF-2, and CMF-7. The Northridge motion shows the minimum misfit for matched spectral accelerations in CMF-5 and CMF-6. The Loma Prieta motion is applicable for CMF-4, and the Friuli motion is applicable for CMF-3.

Figure 8 presents the spectral accelerations of the minimum misfit spectral acceleration from spectral matching results in Table 2. It can be observed that matching spectral accelerations are generally consistent with targeted spectral acceleration for sites. Spectral accelerations are also compared to the seismic design code for West Java Province, i.e. SNI 1726:2019 (2019). It is observed that spectral acceleration for seismic design code is still higher than matched spectral acceleration. If the structural buildings in the study area are designed based on seismic design code, the buildings could be relatively more resistant to earthquake shaking.

Figure 9 presents the time history of acceleration for each investigated site. In Fig. 9, it can be observed that the time history of matched spectral acceleration (red line) is generally consistent with the time history of recorded ground motion (blue line). For CMF-1, PGA for input motion is 0.043 g, whereas the input motion for CMF-2 is about 0.033 g. For CMF-2, CMF-4, and CMF-5, PGA values for the input motions are 0.023 g, 0.044 g, and 0.135 g, respectively. For CMF-6 and CMF-7, the input motions are 0.033 g and 0.042 g, respectively. PGA values obtained from the spectral matching method are then used as the input motion for one-dimensional seismic ground response analysis.

4.2 Ground responses

4.2.1 Acceleration profiles

The results of one-dimensional seismic ground response analysis in terms of acceleration profiles are presented in this study. Figure 10 presents the acceleration profiles for the investigated sites. It can be observed PGA values at the ground surface are observed to vary from 0.031 to 0.191 g. The minimum PGA at the ground surface is recorded at CMF-1 with a value of about 0.031 g, whereas the maximum one is recorded at CMF-5 with a value of 0.191 g. As previously elaborated, CMF-3 is the farthest site to the earthquake epicentre, and CMF-5 is the closest site to the earthquake epicentre. For input motion, the values of PGA input vary from 0.023 to 0.135 g. Therefore, ground motion amplification could occur during seismic wave propagation.

Table 2 Summary of misfits from spectral matching results

Sites	Ground motions	Matching condition	Average misfit
CMF-1	Kobe	Converged	0.032
	Loma Prieta	Converged	0.055
	Imperial Valley	Non-converged	0.083
	Northridge	Converged	0.053
CMF-2	Friuli	Converged	0.071
	Kobe	Converged	0.020
	Loma Prieta	Non-converged	0.113
	Imperial Valley	Converged	0.045
CMF-3	Northridge	Converged	0.069
	Friuli	Converged	0.025
	Kobe	Non-converged	0.037
	Loma Prieta	Non-converged	0.125
CMF-4	Imperial Valley	Non-converged	0.037
	Northridge	Converged	0.031
	Friuli	Converged	0.024
	Kobe	Non-converged	0.072
CMF-5	Loma Prieta	Converged	0.027
	Imperial Valley	Converged	0.051
	Northridge	Non-converged	0.155
	Friuli	Non-converged	0.068
CMF-6	Kobe	Non-converged	0.030
	Loma Prieta	Non-converged	0.043
	Imperial Valley	Non-converged	0.038
	Northridge	Converged	0.021
CMF-7	Friuli	Converged	0.036
	Kobe	Converged	0.049
	Loma Prieta	Converged	0.051
	Imperial Valley	Non-converged	0.184
CMF-8	Northridge	Converged	0.022
	Friuli	Converged	0.037
	Kobe	Converged	3.40%
	Loma Prieta	Converged	3.40%
CMF-9	Imperial Valley	Non-converged	11.10%
	Northridge	Non-converged	13.20%
	Friuli	Converged	3.30%
	Kobe	Converged	3.30%

Bold value indicates the minimum average misfit

Based on one-dimensional seismic ground response analysis, there are three main trends of seismic wave propagation in the study area. For CMF-2 (Fig. 10b) and CMF-4 (Fig. 10d), the seismic wave propagation tends to enlarge gradually through layers up to the ground surface. This may cause by the existence of low soil resistance in the soil layers. For CMF-1 (Fig. 10a), CMF-3 (Fig. 10c) and CMF-6 (Fig. 10f), the maximum acceleration of layers tends to constantly propagate through the layer at the middle depth and significantly increase for the middle depth to the ground surface. According to Yoshida (2015)

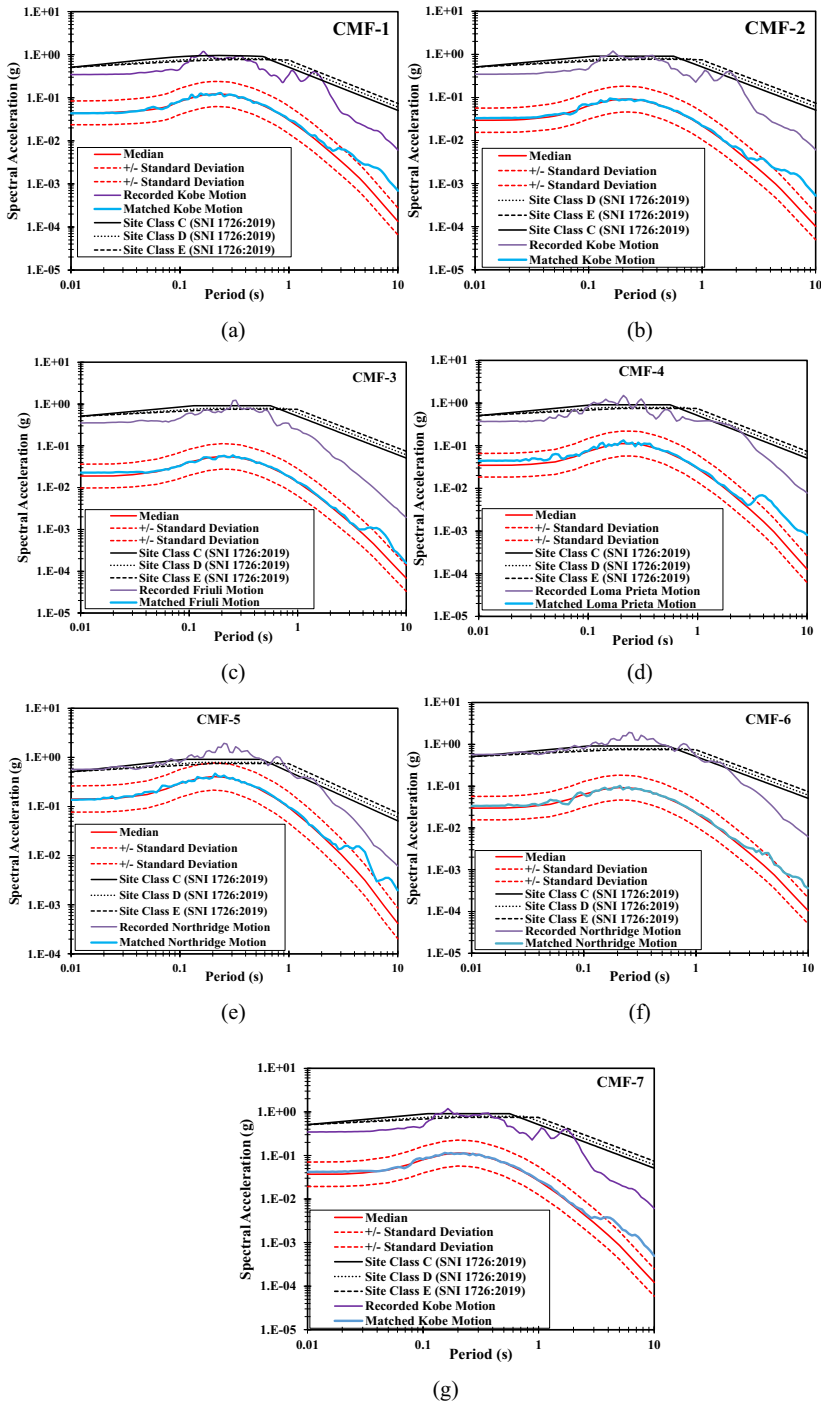


Fig. 8 Spectral matching results comparison for a CMF-1, b CMF-2, c CMF-3, d CMF-4, e CMF-5, f CMF-6, g CMF-7

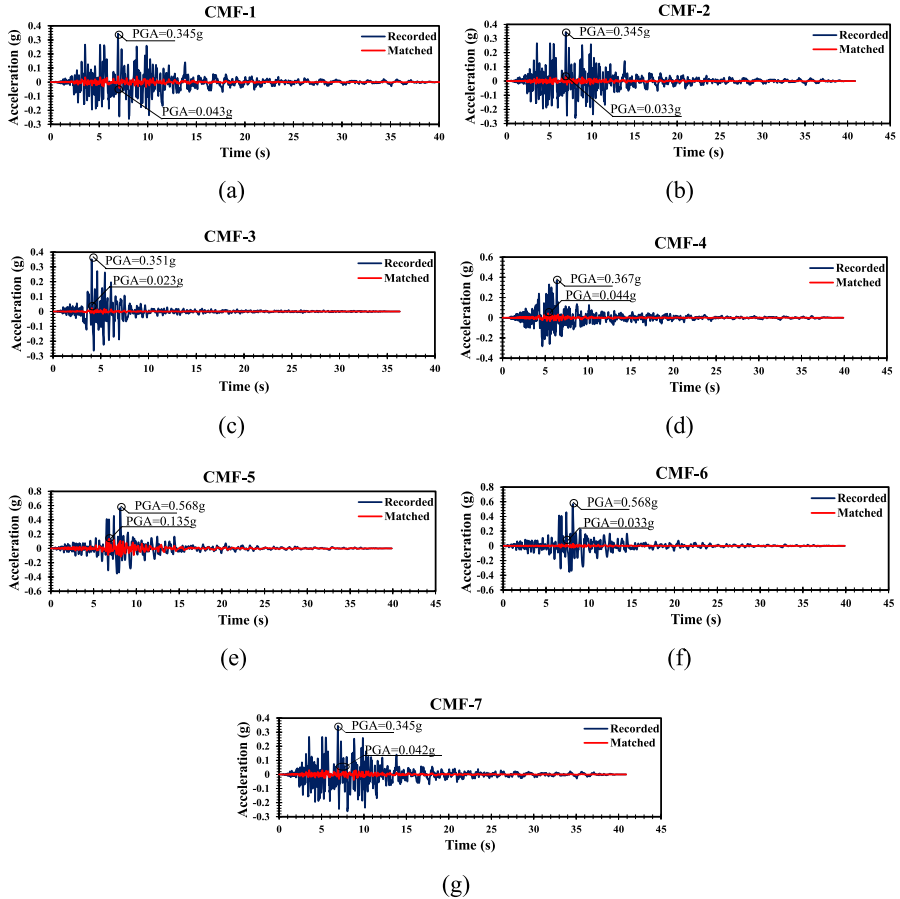


Fig. 9 Comparison of motions between the recorded ground motion and the matched input motion for **a** CMF-1, **b** CMF-2, **c** CMF-3, **d** CMF-4, **e** CMF-5, **f** CMF-6, **g** CMF-7

and Mase et al. (2018), the weak layer generally controls the amplification of peak ground acceleration. In this case, several sand layers with relatively high-soil resistance (V_{s30} and SPT-N) in those sites are important in reducing the maximum PGA value in the middle depth. The maximum PGA values vary according to depth for CMF-5 (Fig. 10e) and CMF-7 (Fig. 10g). Based on the observation, there is amplification and de-amplification of maximum acceleration in the investigated depth. The existence of various sand layers with various soil resistance at the middle depth could influence the maximum acceleration of propagated wave.

The more considerable soil resistance, the smaller the maximum acceleration and vice versa. In general, near ground surface to the ground surface, the maximum PGA value increases. Based on site investigation, the ground motion could increase near the ground surface. This is because the shear strength of the weak layer dominated by clayey sand control the amplification (Finn et al. 1978). Therefore, the ground motion enlarges to the

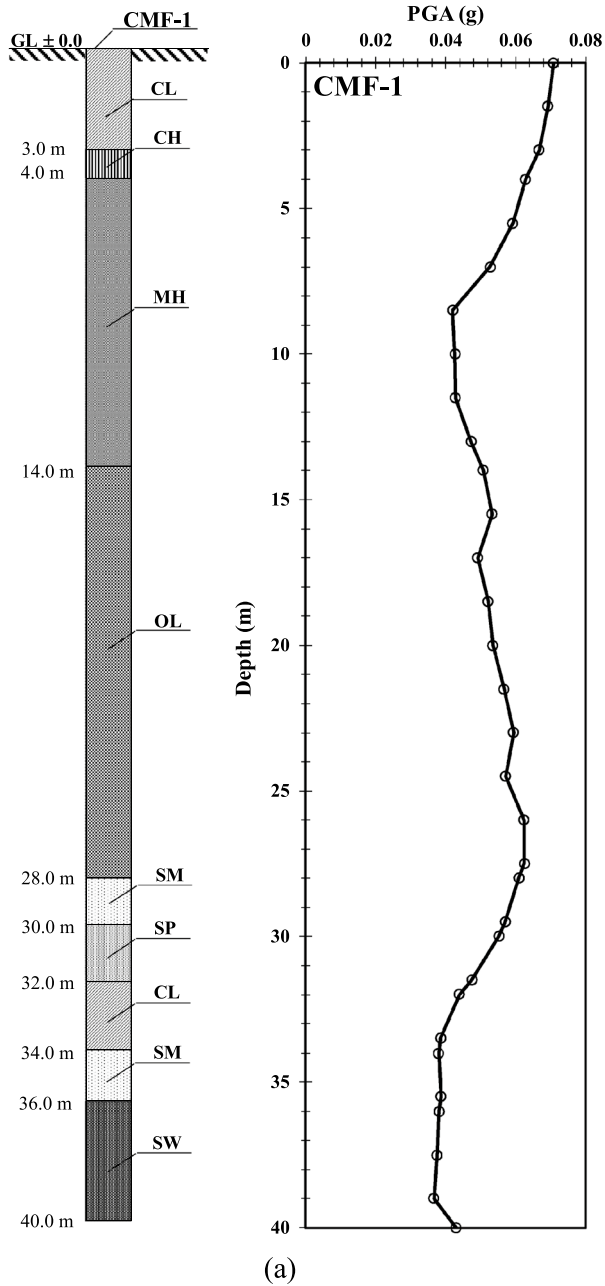
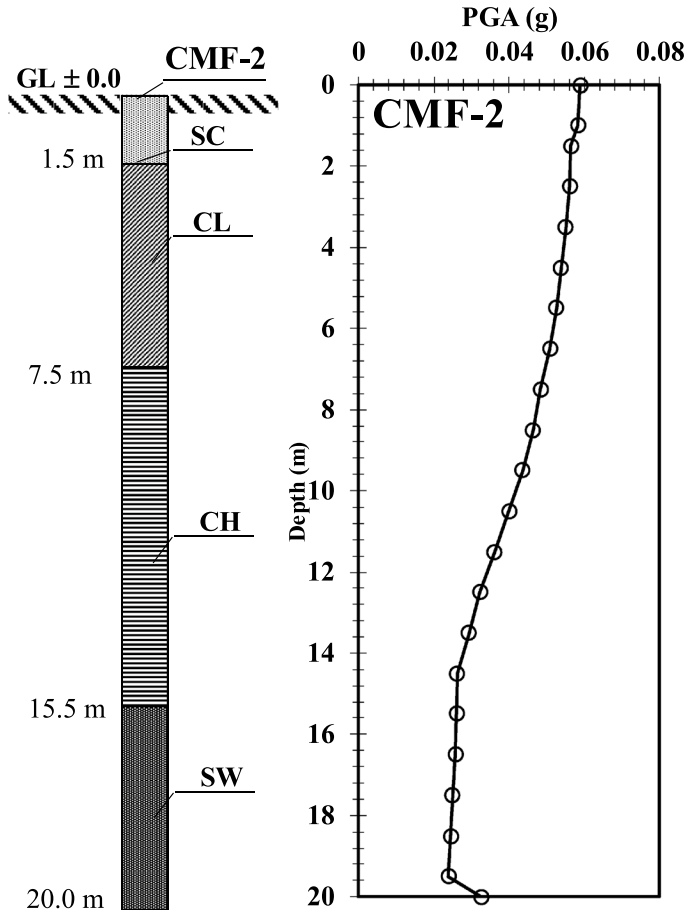


Fig. 10 Profiles of acceleration from one-dimensional of seismic ground response analysis a CMF-1, b CMF-2, c CMF-3, d CMF-4, e CMF-5, f CMF-6, and g CMF-7



(b)

Fig. 10 (continued)

ground surface. Based on the analysis results, a clay layer near the surface could amplify propagated ground motion in the study area.

4.2.2 Time history of accelerations and spectral accelerations at the surface

Figure 11 presents the time history of accelerations and spectral accelerations at the ground surface. It can be observed that for CMF-1 (Fig. 11a); CMF-2 (Fig. 11b); CMF-3 (Fig. 11c), PGA values at the ground surface are generally less than 0.05 g. The locations of those sites are relatively far from the epicentre, i.e. about 40–75 km. (Regnier et al. 2013) mentioned that to observe the significance of the amplification effect and resonance possibility, the spectral acceleration comparison could be performed. In terms of spectral acceleration comparison, it can be observed that both spectral accelerations at the ground surface and input motion are lower than the designed spectral acceleration. In other words,

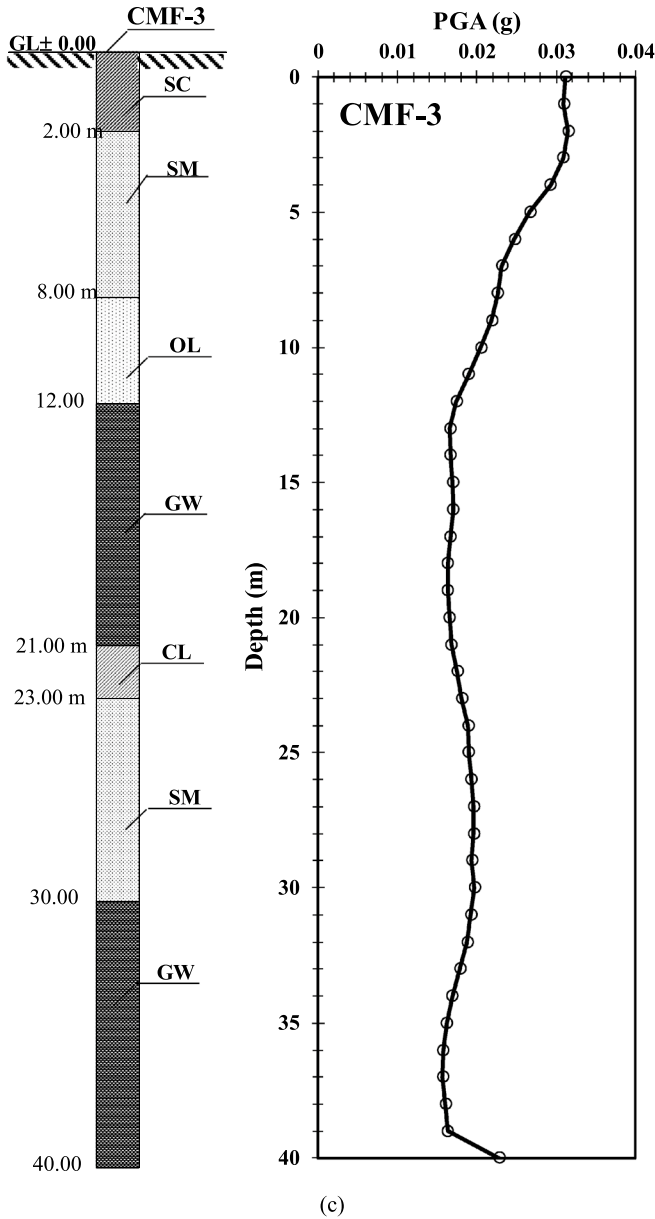
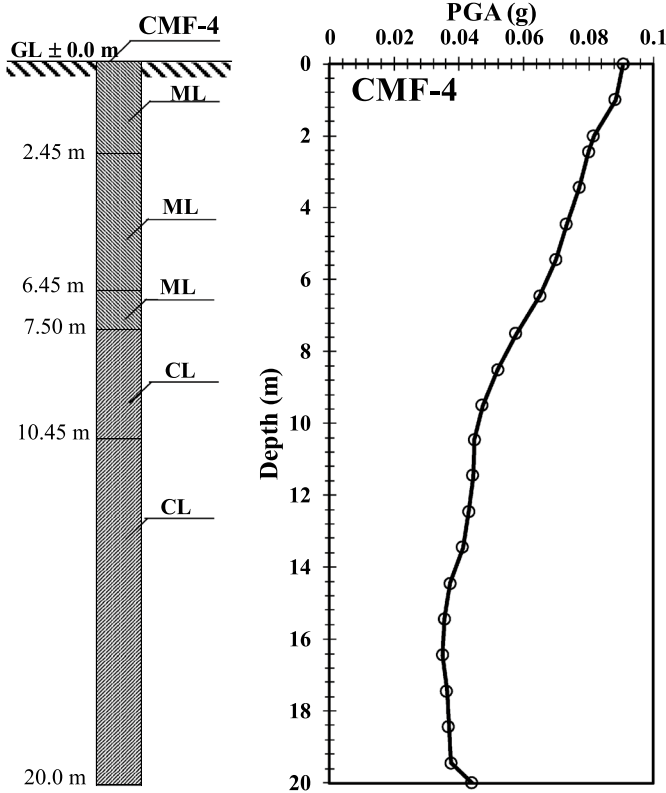


Fig. 10 (continued)

it can be roughly estimated that buildings following the designed spectral acceleration in both plan and construction are relatively more resistant to the effect of earthquake shaking.

For CMF-4 (Fig. 11d); CMF-6 (Fig. 11f); and CMF-7 (Fig. 11g), PGA values are in the range of 0.05–0.01 g. Those sites are generally located within a 46–56 km radius of the epicentre. Generally, those sites’ PGA values at the surface are relatively more significant



(d)

Fig. 10 (continued)

than the input motion. It indicates that there is an amplification of PGA at those sites. Regarding spectral acceleration comparison, spectral accelerations for input motion and at-the-ground response are generally lower than seismic design code. It simply explains that the seismic resistance design based on Indonesian Seismic Design Code (SNI 1726:2019) tends to provide better seismic resistance for buildings following the code during the earthquake in 2022.

For CMF-5 (Fig. 11e), PGA at the ground surface is about 0.191 g. CMF-5 has the largest PGA at the ground surface among the investigated sites during seismic wave propagation. It is because of the site's position, which is close to the earthquake epicentre. It is also observed that there is an indication of PGA amplification during the strong earthquake. This is because PGA at the ground surface is larger than the PGA of input motion. Figure 10e shows that the ground surface's spectral acceleration is close to the designed spectral acceleration in the short period, especially for Site Classes D and E. It can be roughly concluded that the seismic resistance design could be exceeded by spectral acceleration at the ground surface if a stronger earthquake happens. Therefore, the results of this study

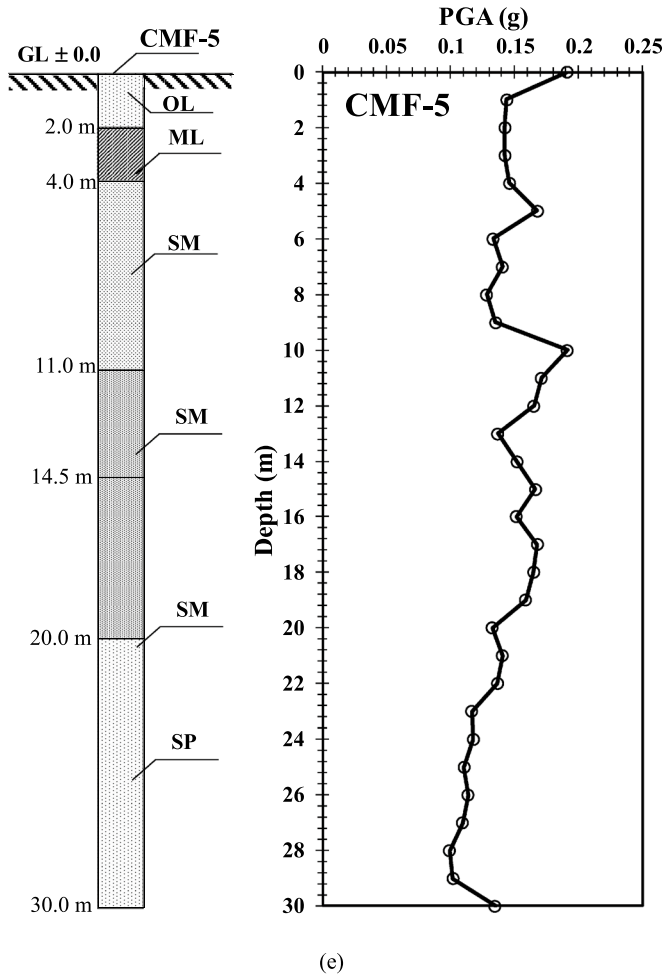


Fig. 10 (continued)

could suggest the updated seismic design code for building construction to reduce potential seismic damage in the area.

4.2.3 PGA amplification factor

Figure 12 presents each investigated site’s PGA amplification factor (AF). Figure 12 shows that the amplification factor of PGA during seismic wave propagation is observed to vary from 1.37 to 2.06. Generally, the average PGA in the study area is about 1.8. CMF-6 has the largest AF among all studied areas, i.e. 2.06 and CMF-3, with an AF of 1.37, has the smallest AF among all studied areas. Based on the site investigation data, CMF-6 has a significant variation in soil resistance, especially from the depth of 12 to the ground surface, as presented in Fig. 4f.

Ezzelarab et al. (2018) suggested that geological conditions could influence the amplification factor. As elaborated by Mase et al. (2018), the amplification of peak ground

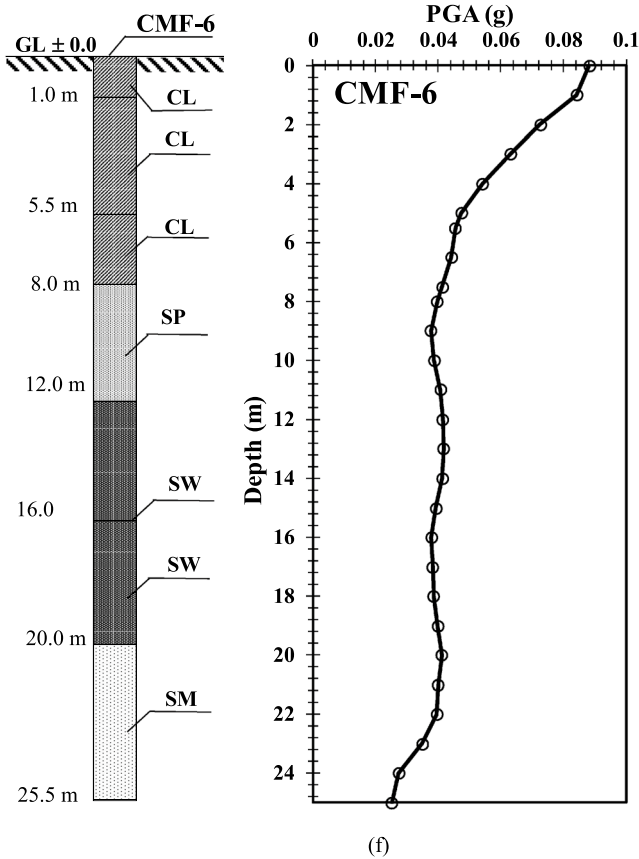


Fig. 10 (continued)

acceleration at the ground surface depends on the shear strength of the weaker layer. In CMF-6, the weak layer is generally found in the clay layer having low SPT-N. Therefore, the PGA value could amplify at the ground surface during seismic wave propagation. For CMF-3, the lower amplification factor could be influenced by soil resistance. As presented in Fig. 4c, the variation of soil resistance in terms of SPT-N for CMF-3 is insignificant. In addition, there are sand layer deposits at shallow depths. Since these sand layers tend to have more soil resistance than clay layers in other sites. Therefore, the amplification of PGA in this site could be more significant.

Joseph et al. (2021) explained that ground motion could influence the amplification factor besides geological conditions and site characteristics. In this study, minor PGA input (less than 0.1 g) means a larger amplification factor, as shown in CMF-1 to CMF-4 and CMF-7. For CMF-5, the input motion is about 0.1 g, and the amplification factor is recorded as 1.42. Qodri et al. (2021) also mentioned that soil response for minor input motion during seismic wave propagation is still linear, so the amplification factor is relatively larger. Since the soil response is still linear for a small PGA input, the damping effect is not significantly increasing; therefore, the amplification factor of PGA could be larger

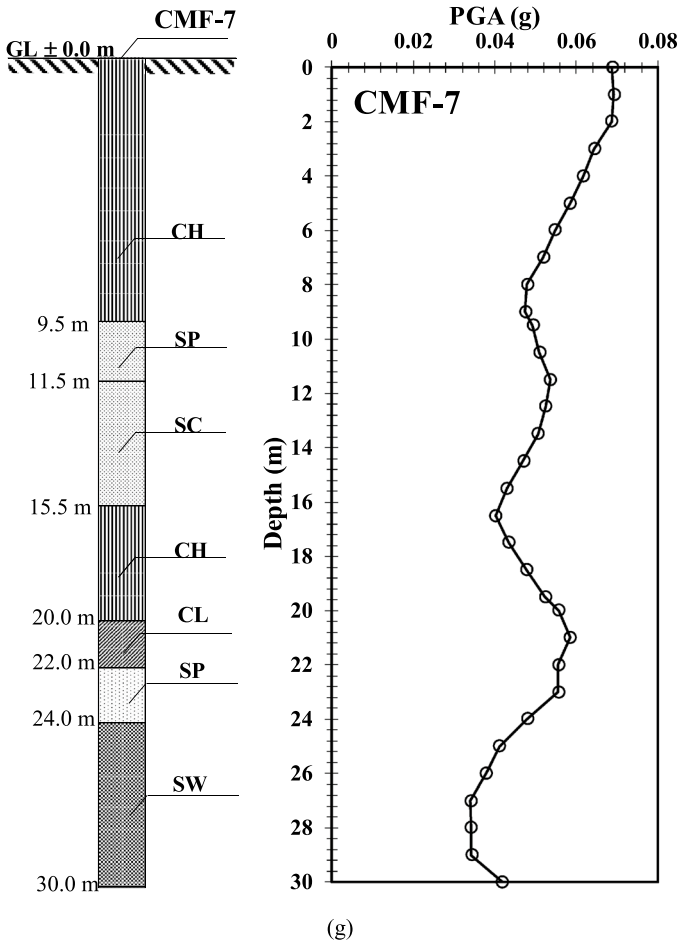


Fig. 10 (continued)

(Roten et al. 2009). Based on the analysis results, it can be concluded that the amplification factor in the investigated sites could be influenced by the input motion’s PGA and geological characteristics.

Several studies of seismic ground response analysis in two or three-dimensional suggested that the topography effect could play an essential role in determining seismic amplification. Stone et al. (2022) suggested that average ground motions in simulations with and without topography are similar. However, shaking amplification is common at topographic highs, which is also previously suggested by Massa et al. (2014). A case by Dunham et al. (2022) mentioned that the largest landslides that occurred during the 2015 Gorkha Earthquake, generated were due to the highest topographic amplification, highest elevations, and steepest slopes converged. It may indicate that soil response during earthquakes could be high in topography areas. Therefore, the influence of topographic amplification should be considered in determining ground motion prediction. Unlike amplification due to soil conditions in ground motion prediction formulas, topographic effects are generally less considered. This may be because there are some significant practical difficulties in

Fig. 11 Time-history of accelerations and spectral accelerations based on one-dimensional seismic ground response analysis for **a** CMF-1, **b** CMF-2, **c** CMF-3, **d** CMF-4, **e** CMF-5, **f** CMF-6, and **g** CMF-7

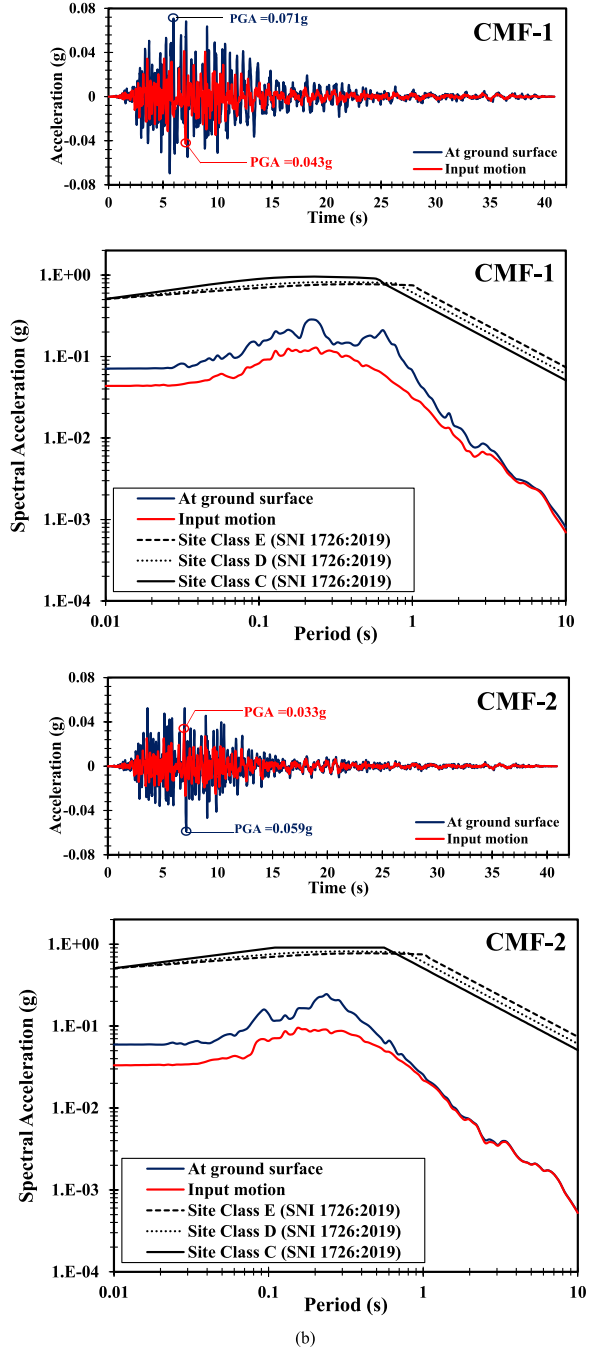


Fig. 11 (continued)

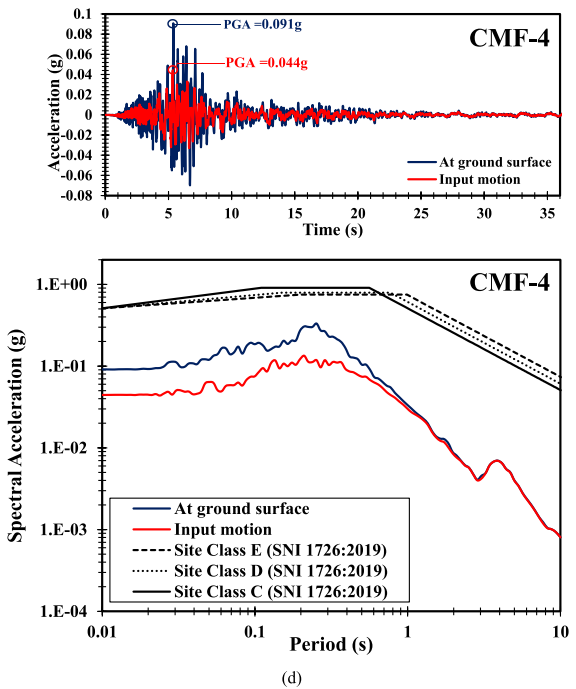
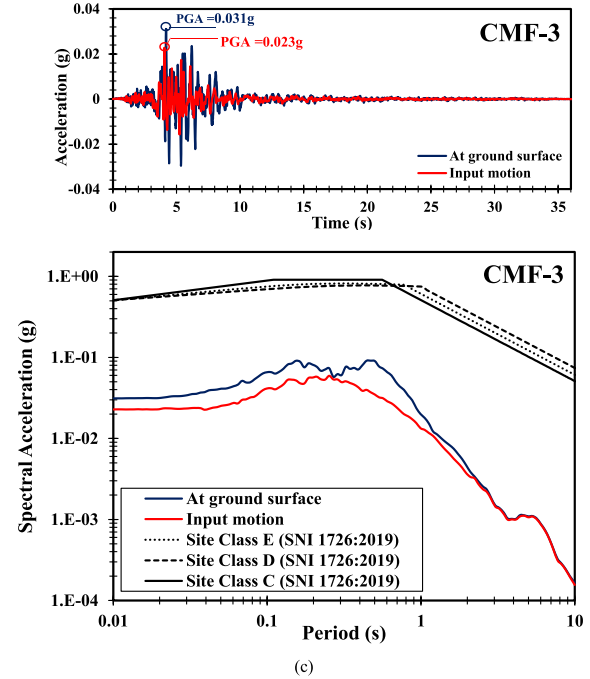
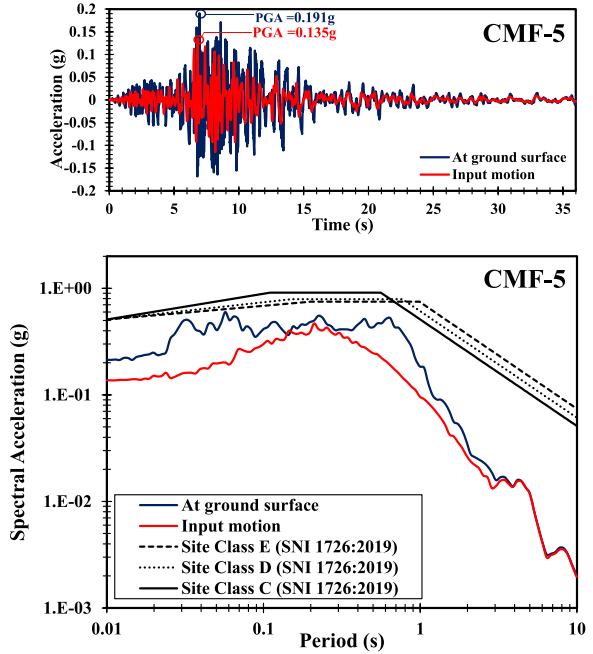
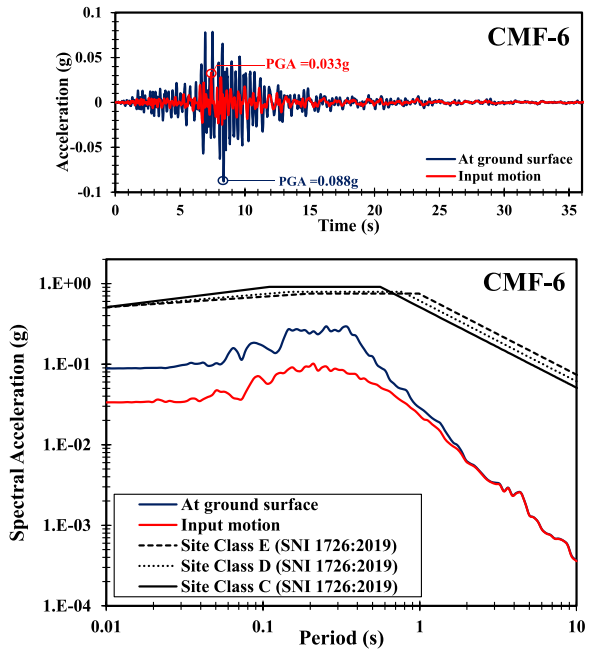


Fig. 11 (continued)



(e)



(f)

Fig. 11 (continued)

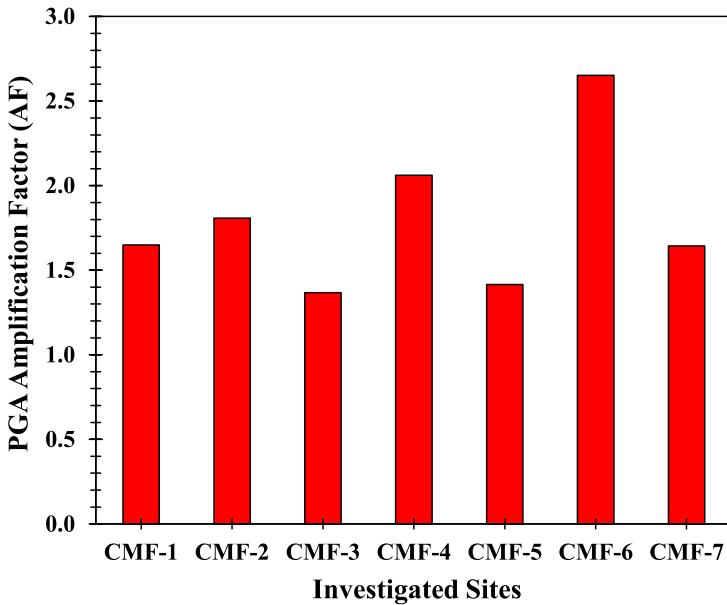
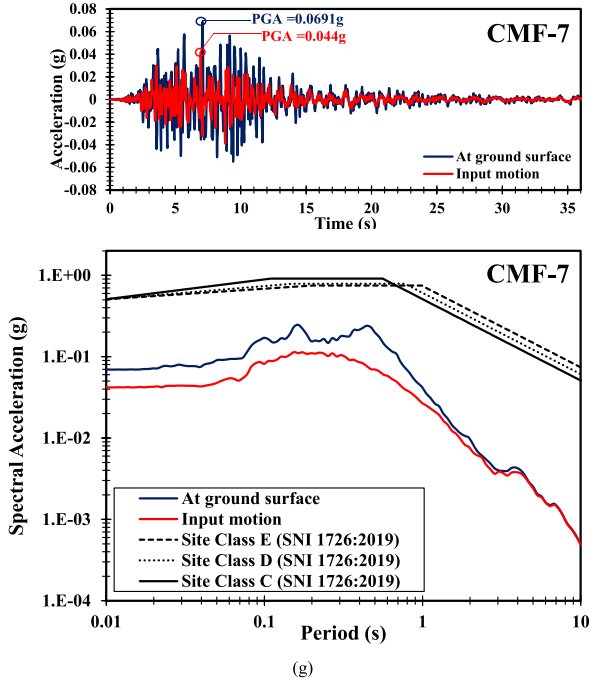


Fig. 12 PGA amplification factor for the investigated sites

introducing them into ground motion prediction, including inherent difficulties in reliably determining the level of topographic amplification, the lack of an exhaustive classification of topographic irregularities, the lack of recorded data and the definition of effective predictors (Barani et al. 2014). Since this study area is generally surrounded by hills, slopes, and valleys that can influence the seismic ground response, the effect of topography on seismic amplification during the Cianjur Earthquake under two or three-dimensional seismic ground response analysis will be discussed in further study.

4.3 Potential seismic damage to structures

PGA values could also be used to predict the seismic damage level during an earthquake. Figure 13 presents the prediction of damage intensity level in the study area. Linkimer (2008) states that a larger PGA means a more significant damage intensity level. In Fig. 13, it can be observed that the MMI level that could occur in the study area during the earthquake is observed to vary from Scale VI (Strong) to Scale VIII (Severe). According to Elnashai and Di Sarno (2015) and Tjockrodimaljo (2000), Scale VI reveals “*Felt by all, and many are frightened. Some heavy furniture is moved; a few instances of fallen plaster occur. Damage is slight.*”. Scale VII reveals, “*Damage is negligible in buildings of good design and construction, but slight to moderate in well-built ordinary structures; damage is considerable in poorly built or badly designed structures; some chimneys are broken. Noticed by motorists.*”. Scale VIII reveals “*Damage slight in specially designed structures; considerable damage in ordinary substantial buildings with partial collapse. Damage is great in poorly built structures, the fall of chimneys, factory stacks, columns, monuments,*

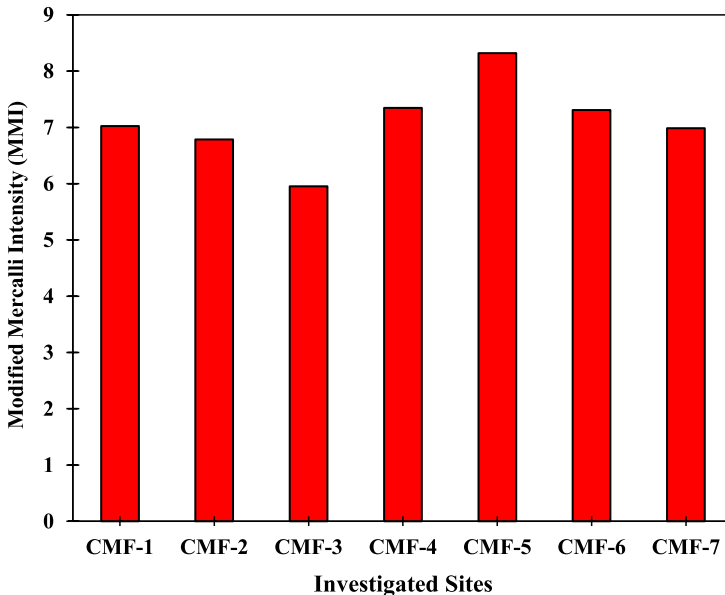


Fig. 13 Modified Mercalli Intensity for the investigated sites

Table 3 Historical moderate earthquakes occurred in West Java, with the epicentre located on land (National Agency for Disaster Countermeasure 2023)

Date	Earthquakes	Earthquake types	Predicted triggering fault	Mag-nitude (M_w)	Latitude (S)	Longitude (E)	Focal depth (km)	MMI Level
13 January 2001	The Ciamis-Kuningan Earthquake	Shallow Crustal Earth-quake	Ciremai Fault	5.1	7° 13' 52.22" S	108° 29' 4.67" E	10	III–VI
25 October 2020	The Sukabumi Earth-quake	Shallow Crustal Earth-quake	Cipamingkis Fault	5.1	6° 53' 24.00" S	106° 37' 12.00" E	12	III–VI
21 November 2022	The Cianjur Earthquake	Shallow Crustal Earth-quake	Cimandiri Fault	5.6	6° 51' 10.80" S	107° 05' 42.00" E	10	III–VIII
3 December 2022	The Garut Earthquake	Shallow Crustal Earth-quake	Indo-Australia Plate (Intraslab)	6.4	7° 26' 24.00" S	107° 30' 36.00" E	109	II–V

and walls. Heavy furniture overturned. Sand and mud are ejected in small amounts. Changes in well water occur. Motorists are disturbed’.

The Cianjur Earthquake’s impact and characteristics are also compared to several earthquakes in West Java, especially on land, as presented in Table 3. In Table 3, several historical earthquakes with moderate magnitude that occurred in West Java are compiled. Earthquakes called the Ciamis-Kuningan Earthquake that occurred in 2001 could result in a damage intensity level (MMI) of about III-VI, with Ciamis and Kuningan as two regions that underwent significant impact. The Sukabumi Earthquake in 2020, just two years before The Cianjur Earthquake occurred, is also reported as the most devastating earthquake after the Ciamis-Kuningan Earthquake in 2001. The earthquake-triggered damage intensity levels varied from III to VI. Another recent earthquake called The Garut Earthquake which was triggered by the activity of intraslab (Indo-Australia plate), has also resulted in low significant damage, i.e. about II to IV on the MMI scale. Among those historical and recent earthquakes, the Cianjur Earthquake recorded the highest damage intensity, consistent with the prediction explained in the previous paragraph.

Generally, the distance between the epicentre to the investigated site could influence PGA (Fig. 14). As presented in Fig. 14, a further distance means a minor MMI level. In line with this, it can be roughly estimated that sites located within a radius of 40–60 km from the epicentre could undergo an MMI scale up to VII, whereas sites located within 15–40 km from the epicentre could undergo an MMI scale up to VIII. A site within a more than 60 km radius could undergo an MMI scale up to VI.

Figure 15 presents the correlation between MMI level and V_{s30} for each investigated site. In Fig. 15, it can be generally observed that the smaller V_{s30} means the larger MMI scale. According to Mase et al. (2021b), V_{s30} could be important in determining seismic vulnerability. Areas having lower V_{s30} could undergo more significant damage than areas with higher V_{s30} . V_{s30} , the parameter representing the site effect, is also used for ground motion prediction (Liu et al. 2013). Several studies conducted by Ornthammarath (2013),

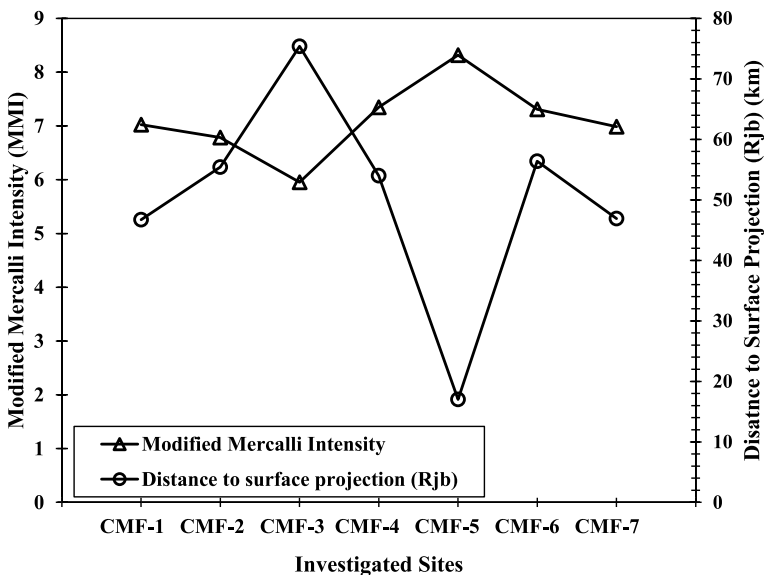


Fig. 14 Correlation between MMI and R_{jb}

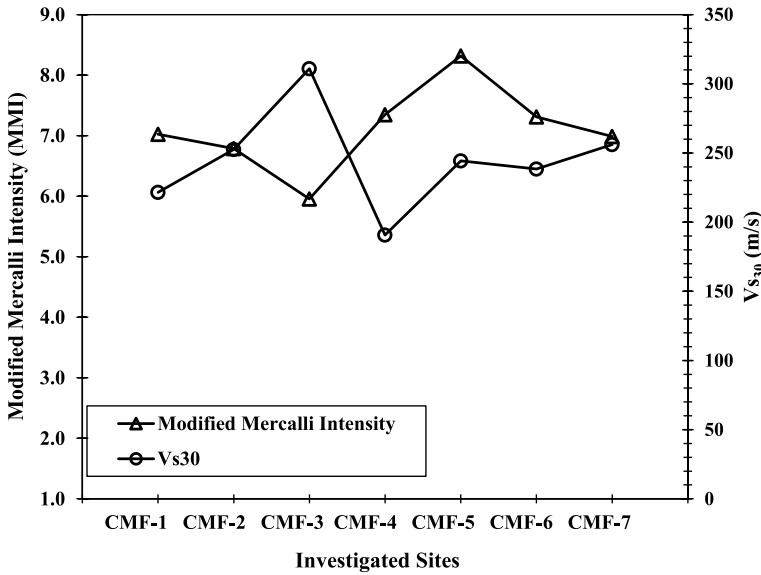


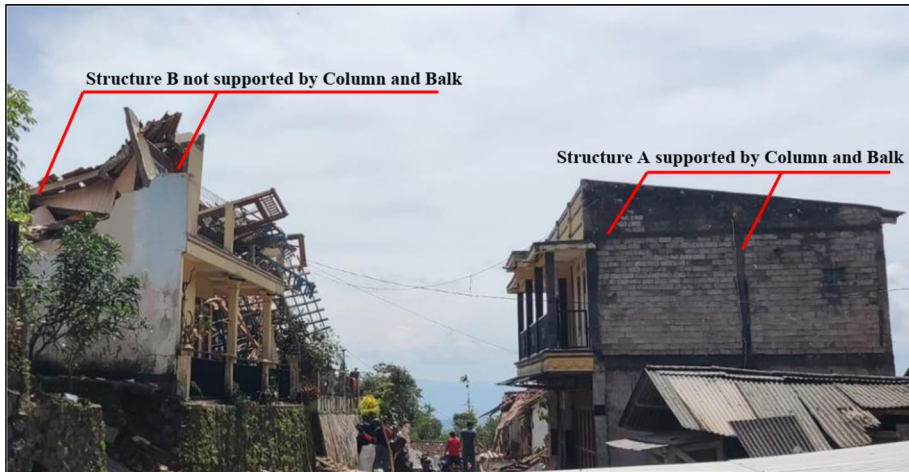
Fig. 15 Correlation between MMI and V_{s30}

Mase (2019), and Mase et al. (2020) had confirmed that the role of V_{s30} is important in determining the PGA. Therefore, V_{s30} could also influence the damage intensity level in the study area. For structural design in the study area, the site-specific analysis considering the detailed analysis of geotechnical and geophysical aspects should be carefully conducted before construction.

4.4 Prediction and field evidence

The results also show that CMF-3 could undergo damage with the intensity level of Scale VI. For CMF-1, CMF-2, CMF-4, CMF-6, and CMF-8, the damage intensity level is Scale VII. CMF-5 could undergo damage intensity of Scale VIII. In terms of spectral acceleration presented in Fig. 11, all spectral accelerations based on seismic ground response analysis are generally lower than the seismic design code. Based on a reconnaissance report from Burton et al. (2022), the damage during the Cianjur Earthquake was massive, especially in areas within 30 km from the epicentre. Scale VIII of MMI suggested that the damage is categorised as slight for the designed structures. The damage to the structure is very massive as shown in Fig. 16. In Fig. 16a, it can be observed that two neighbouring structures are in the same area. Structure A, constructed following the seismic resistance standard with a balk and column, experienced relatively minimal damage compared to Structure B without columns and balks. In Fig. 16b, the lightweight structure tends to have minor damage compared to the heavy-weight structure. Both structures are located in the same area. A simple structure with a symmetric form is more relatively resistant than a complex structure with additional mass as building accessories (Chopra et al. 1972; Michiels and Adriaenssens 2017).

Based on the analysis and field evidence, it can be concluded that many buildings in the study area, especially those within a 30 km radius of the epicentre, might not implement



(a)



(b)

Fig. 16 Damage due to the Cianjur Earthquake in November 2022 (Project Hope 2022): **a** comparison of damage for structures with and without balk and column, **b** significant damage difference between light structure and heavy structure

and follow the seismic design code. Implementing these codes has always been challenging due to economic, regional, and other factors. Specifically, large structures in rural areas, especially for residential housing, were constructed without consideration of the building codes and are often non-engineered, resulting in severe damage to buildings when an

earthquake occurs Burton et al. (2022). Overall, the results of this study suggest that the local government enforce the implementation of a seismic design code to minimise the potential seismic damage in the study area.

5 Concluding remarks

This paper analyses ground response and the potential seismic damage to structures in Sites Surrounding Cimandiri Fault, West Java, Indonesia, during the recent earthquake event, i.e. the M_w 5.6 Cianjur Earthquake in 2022. Site investigation and one-dimensional seismic ground response analysis are conducted. The prediction of ground motion and damage intensity level is performed. Several concluding remarks can be drawn:

1. The investigated sites surrounding the Cimandiri Fault are generally dominated by clay and sand layers. The significant difference in soil resistance could also influence the amplification of PGA. A clay layer with low soil resistance at shallow depths could amplify PGA at the ground surface.
2. The distance could strongly influence the damage intensity level in the study area to the earthquake source and the site condition.
3. Generally, the spectral acceleration from the seismic design code could provide a more resistant design for structural buildings in the study area. Therefore, the seismic design code should be implemented to minimise significant damage during a strong earthquake in the study area
4. The damage intensity level shows that the effect of an earthquake could be significant for buildings that do not implement the seismic design code. Implementing seismic resistance design could be challenging because of several aspects, such as social-economic factors. Therefore, this study would suggest that local government consider the building permit before construction. In addition, seismic design code should be implemented for areas with high-seismic vulnerability.
5. Topography features can influence the ground response, especially amplification. Hills, slopes, and valleys surround the study area, and these topography conditions can influence the amplification. More data, including 2D and 3D geological modelling, should be collected to support an advanced study in observing the topographical effect on ground response. The detail will be presented in further study.

Acknowledgements This study is conducted in collaboration between the University of Bengkulu, the National Research and Innovation Agency, King Mongkut's Institute of Technology Ladkrabang, and Bandung State Polytechnics. This study is also partially supported by the Visiting Researcher Batch 3 program from the National Research and Innovation Agency (BRIN), Indonesia, with contract reference no. 15/III/HK/2023. The Authors also would like to thank everyone who contributed to this research.

Author contributions All authors contributed to the study conception and design, material preparation, data collection and analysis, and the first draft of the manuscript, and all authors commented on previous versions. All authors read and approved the final manuscript.

Funding The authors declare that no funds, grants, or other support was received during the preparation of this manuscript.

Data availability All the datasets used and analysed during the current study are available from the corresponding author upon reasonable request.

Declarations

Conflict of interest The authors declare that they have no conflict of interest.

References

- Abrahamson NA, Silva WJ, Kamai R (2014) Summary of the ASK14 ground motion relation for active crustal regions. *Earthq Spectra* 30(3):1025–1055. <https://doi.org/10.1193/070913EQS198>
- Adampira M, Alielah H, Panji M, Koohsari H (2015) Comparison of equivalent linear and nonlinear methods in seismic analysis of liquefiable site response due to near-fault incident waves: a case study. *Arab J Geosci* 8:3103–3118. <https://doi.org/10.1007/s12517-014-1399-6>
- Ademovic N, Hadzima-Nyarko M, Zagora N (2022) Influence of site effects on the seismic vulnerability of masonry and reinforced concrete buildings in Tuzla (Bosnia and Herzegovina). *Bull Earthq Eng* 20(5):2643–2681. <https://doi.org/10.1007/s10518-022-01321-2>
- Barani S, Massa M, Lovati S, Spallarossa D (2014) Effects of surface topography on ground shaking prediction: implications for seismic hazard analysis and recommendations for seismic design. *Geophys J Int* 197(3):1551–1565. <https://doi.org/10.1093/gji/ggu095>
- Bessette C, Yniesta S (2023) Assessment of the prediction of ground motion parameters in 1D ground response analysis using data from seismic arrays and centrifuge experiments. *Earthq Spectra*. <https://doi.org/10.1177/87552930221150828>
- Bisri MB (2013) Examining inter-organizational network during emergency response of West Java earthquake 2009, Indonesia. *Procedia Environ Sci* 17:889–898. <https://doi.org/10.1016/j.proenv.2013.02.107>
- Boore DM, Stewart JP, Seyhan E, Atkinson GM (2014) NGA-West2 equations for predicting PGA, PGV, and 5% damped PSA for shallow crustal earthquakes. *Earthq Spectra* 30(3):1057–1085. <https://doi.org/10.1193/070113EQS184M>
- Bozorgnia Y, Abrahamson NA, Al Atik L, Ancheta TD, Atkinson GM, Baker JW et al (2014) NGA-West2 research project. *Earthq Spectra* 30(3):973–987. <https://doi.org/10.1193/072113EQS209M>
- Burton H, Dwima S, Gho D, Guan X, Gunay S, Gupta A, Khalil Z, Kusumayani N, Marinkovic M, Merino-Pena Y, Nweke C, Safey A (2022) Preliminary Virtual Reconnaissance Report. Structural Extreme Events Reconnaissance (StEER). <https://doi.org/10.17603/ds2-e2vq-nq61>
- Campbell KW, Bozorgnia Y (2014) NGA-West2 ground motion model for the average horizontal components of PGA, PGV, and 5% damped linear acceleration response spectra. *Earthq Spectra* 30(3):1087–1115. <https://doi.org/10.1193/062913EQS175M>
- Chiou BSJ, Youngs RR (2014) Update of the Chiou and Youngs NGA model for the average horizontal component of peak ground motion and response spectra. *Earthq Spectra* 30(3):1117–1153. <https://doi.org/10.1193/072813EQS219M>
- Chopra AK, Chakrabarti P (1972) The earthquake experience at Koyna dam and stresses in concrete gravity dams. *Earthq Eng Struct Dynam* 1(2):151–164. <https://doi.org/10.1002/eqe.4290010204>
- Dolce M, Masi A, Marino M, Vona M (2003) Earthquake damage scenarios of the building stock of Potenza (Southern Italy) including site effects. *Bull Earthq Eng* 1:115–140. <https://doi.org/10.1023/A:1024809511362>
- Duncan JM, Chang CY (1970) Nonlinear analysis of stress and strain in soils. *J Soil Mech Found Division, ASCE* 96(5):1629–1653. <https://doi.org/10.1061/JSEFAQ.0001458>
- Dunham AM, Kiser E, Kargel JS, Haritashya UK, Watson CS, Shugar DH et al (2022) Topographic control on ground motions and landslides from the 2015 Gorkha earthquake. *Geophys Res Lett* 49(10):e2022GL098582. <https://doi.org/10.1029/2022GL098582>
- Elnashai AS, Di Sarno L (2015) *Fundamentals of earthquake engineering: from source to fragility*. Wiley, Hoboken
- Ezzelarab M, El-Hussain I, Mohamed AM, Deif A (2018) Site-specific earthquake ground motion parameters at the southeastern part of Muscat, Sultanate of Oman. *J Afr Earth Sc* 145:201–214. <https://doi.org/10.1016/j.jafrearsci.2018.05.020>
- Febriani F (2016) Seismicity around the Cimandiri Fault Zone, West Java, Indonesia. In: AIP Conference proceedings (Vol. 1711, No. 1, p. 070003). AIP Publishing LLC. <https://doi.org/10.1063/1.4941644>
- Finn WD, Lee MK, Martin GR (1978) Comparison of dynamic analyses for saturated sands. In *Proc of earthquake engineering and soil dynamics*, ASCE (pp. 472–491)
- Geological Research and Development Centre (2023) Geological map of western Java. Centre of Geological Survey, Indonesia

- Gülerce Z, Kamai R, Abrahamson NA, Silva WJ (2017) Ground motion prediction equations for the vertical ground motion component based on the NGA-W2 database. *Earthq Spectra* 33(2):499–528. <https://doi.org/10.1193/121814EQS213M>
- Gunawan E, Widiantoro S (2019) Active tectonic deformation in Java, Indonesia inferred from a GPS-derived strain rate. *J Geodyn* 123:49–54. <https://doi.org/10.1016/j.jog.2019.01.004>
- Hancock J, Watson-Lamprey J, Abrahamson NA, Bommer JJ, Markatis A, McCoy EMMA, Mendis R (2006) An improved method of matching response spectra of recorded earthquake ground motion using wavelets. *J Earthq Eng* 10(spec01):67–89. <https://doi.org/10.1080/13632460609350629>
- Hashash YMA, Musgrove MI, Harmon JA et al (2020) DEEPSOIL 7, User Manual. Urbana, Board of Trustees of University of Illinois at Urbana-Champaign, IL, USA
- Hashash YM, Park D (2001) Non-linear one-dimensional seismic ground motion propagation in the Mississippi embayment. *Eng Geol* 62(1–3):185–206. [https://doi.org/10.1016/S0013-7952\(01\)00061-8](https://doi.org/10.1016/S0013-7952(01)00061-8)
- Hutchings SJ, Mooney WD (2021) The seismicity of Indonesia and tectonic implications. *Geochem, Geophys, Geosyst* 22(9):e2021GC009812. <https://doi.org/10.1029/2021GC009812>
- Idriss IM (2014) An NGA-West2 empirical model for estimating the horizontal spectral values generated by shallow crustal earthquakes. *Earthq Spectra* 30(3):1155–1177. <https://doi.org/10.1193/070613EQS195>
- Joseph M, Banerjee S, Pakrashi V (2021) Estimation of the dynamic amplification factor at backfill soil behind a gravity wall. *Geotech Res* 8(4):95–107. <https://doi.org/10.1680/jgere.21.00005>
- Likitlersuang S, Plengsiri P, Mase LZ, Tanapalungkorn W (2020) Influence of spatial variability of ground on seismic response analysis: a case study of Bangkok subsoils. *Bull Eng Geol Environ* 79:39–51. <https://doi.org/10.1007/s10064-019-01560-9>
- Linkimer L (2008) Relationship between peak ground acceleration and modified Mercalli intensity in Costa Rica. *Revista Geológica de América Central* (38):81–94
- Liu KS, Tsai YB, Lin PS (2013) A study on fault-type and site-effect (VS30) parameters in the attenuation relationships of peak ground acceleration and peak ground velocity in Ilan, Taiwan, A Study on Fault-Type and Site-Effect Parameters in PGA and PGV in Ilan. *Taiwan Bull Seismol Soci Am* 103(3):1823–1845. <https://doi.org/10.1785/0120120065>
- Marliyani GI, Arrowsmith JR, Whipple KX (2016) Characterization of slow slip rate faults in humid areas: Cimandiri fault zone, Indonesia. *J Geophys Res Earth Surf* 121(12):2287–2308. <https://doi.org/10.1002/2016JF003846>
- Mase LZ (2018) Reliability study of spectral acceleration designs against earthquakes in Bengkulu City, Indonesia. *Int J Technol* 9(5):910–924. <https://doi.org/10.14716/ijtech.v9i5.621>
- Mase LZ (2019) Performance of NGA models in predicting ground motion parameters of the strong earthquake. *J Civil Eng Forum* 5(3):227–242. <https://doi.org/10.22146/jcef.46651>
- Mase LZ (2020) Seismic hazard vulnerability of Bengkulu City, Indonesia, based on deterministic seismic hazard analysis. *Geotech Geol Eng* 38(5):5433–5455. <https://doi.org/10.1007/s10706-020-01375-6>
- Mase LZ, Likitlersuang S, Tobita T (2018) Analysis of seismic ground response caused during strong earthquake in Northern Thailand. *Soil Dyn Earthq Eng* 114:113–126. <https://doi.org/10.1016/j.soildyn.2018.07.006>
- Mase LZ, Likitlersuang S, Tobita T, Chairprakaikeow S, Soralump S (2020) Local site investigation of liquefied soils caused by earthquake in Northern Thailand. *J Earthquake Eng* 24(7):1181–1204. <https://doi.org/10.1080/13632469.2018.1469441>
- Mase LZ, Refrizon R, Anggraini PW (2021a) Local site investigation and ground response analysis on downstream area of Muara Bangkahulu River, Bengkulu City, Indonesia. *Indian Geotech J* 51(5):952–966. <https://doi.org/10.1007/s40098-020-00480-w>
- Mase LZ, Likitlersuang S, Tobita T (2022a) Verification of liquefaction potential during the strong earthquake at the border of Thailand-Myanmar. *J Earthquake Eng* 26(4):2023–2050. <https://doi.org/10.1080/13632469.2020.1751346>
- Mase LZ, Tanapalungkorn W, Likitlersuang S, Ueda K, Tobita T (2022) Liquefaction analysis of Izumio sands under variation of ground motions during strong earthquake in Osaka, Japan. *Soil Found* 62(5):101218. <https://doi.org/10.1016/j.sandf.2022.101218>
- Mase LZ, Yundrismein R, Nursalam MA, Putra SM, Shelina A, Nugroho SH (2022) A study of building performance inspection based on combination of site-specific response analysis and structural analysis (A case study of the Lighthouse View Tower in Bengkulu City, Indonesia). *Rudarsko-geološko-naftni zbornik* 37(3):197–209. <https://doi.org/10.17794/rgn.2022.3.14>
- Mase LZ, Sugianto N, Refrizon (2021b) Seismic hazard microzonation of Bengkulu City, Indonesia. *Geoenviron Disast* 8(1):17. <https://doi.org/10.1186/s40677-021-00178-y>

- Massa M, Barani S, Lovati S (2014) Overview of topographic effects based on experimental observations: meaning, causes and possible interpretations. *Geophys J Int* 197(3):1537–1550. <https://doi.org/10.1093/gji/ggt341>
- Matasovic N (1993) Seismic response of composite horizontally-layered soil deposits. Dissertation, University of California, LA
- Meilano I, Abidin HZ, Andreas H et al (2012) Slip rate estimation of the Lembang Fault West Java from geodetic observation. *J Disaster Res* 7(1):12–18. <https://doi.org/10.20965/jdr.2012.p0012>
- Meteorological, Climatological, and Geophysical Agency (2022). The M_w 5.6 Cianjur Earthquake on 21 November 2022. Meteorological, Climatological, and Geophysical Agency, Indonesia
- Michiels T, Adriaenssens S (2017) Identification of key design parameters for earthquake resistance of reinforced concrete shell structures. *Eng Struct* 153:411–420. <https://doi.org/10.1016/j.engstruct.2017.10.043>
- Misliniyati R, Mase LZ, Irsyam M, Hendriawan H, Sahadewa A (2019) Seismic response validation of simulated soil models to vertical array record during a strong earthquake. *J Eng Technol Sci* 51(6):772–790. <https://doi.org/10.5614/j.eng.technol.sci.2019.51.6.3>
- Mori J, Mooney WD, Kurniawan S et al (2007) The 17 July 2006 tsunami earthquake in West Java, Indonesia. *Seismol Res Lett* 78(2):201–207. <https://doi.org/10.1785/gssrl.78.2.201>
- Muzli M, Kambali RA, Rohadi S et al (2021) MASW for the microzonation of earthquake hazard in Banjar City, West Java, Indonesia. *IOP Conf Series: Earth Environ Sci* 716(1):012032. <https://doi.org/10.1088/1755-1315/716/1/012032>
- National Agency for Disaster Countermeasure (2022) The impact of the M_w 5.6 Cianjur Earthquake, Indonesia. National Agency for Disaster Countermeasure: Indonesia
- National Agency for Disaster Countermeasure (2023). The earthquakes list in West Java, Indonesia. National Agency for Disaster Countermeasure: Indonesia
- National Earthquake Hazards Reduction Program (NEHRP) (1998) Recommended provisions for seismic regulation for new buildings and other structures: part 1-Provisions and Part 2-Commentary, FEMA 302. Texas, USA
- Nugraha AD, Supendi P, Prabowo BS et al (2019) The Recent Small Earthquakes around Lembang Fault, West Java, Bandung, Indonesia. *J Phys: Conf Series* 1204(1):012083. <https://doi.org/10.1088/1742-6596/1204/1/012083>
- Ornthammarath T (2013) A note on the strong ground motion recorded during the M_w 6.8 earthquake in Myanmar on 24 March 2011. *Bull Earthq Eng* 11(1):241–254. <https://doi.org/10.1007/s10518-012-9385-4>
- Paris R, Switzer AD, Belousova M, Belousov A, Ontowirjo B, Whelley PL, Ulvrova M (2014) Volcanic tsunami: a review of source mechanisms, past events and hazards in Southeast Asia (Indonesia, Philippines, Papua New Guinea). *Nat Hazards* 70:447–470. <https://doi.org/10.1007/s11069-013-0822-8>
- Project Hope (2022) The Cianjur, Indonesia Earthquake: What You Need To Know. Retrieved from Project Hope: <https://www.projecthope.org/cianjur-indonesia-earthquake-what-you-need-to-know/11/2022/>. Accessed on 26 Feb 2023
- Qodri MF, Mase LZ, Likitlarsuang S (2021) Non-linear site response analysis of Bangkok subsoils due to earthquakes triggered by Three Pagodas Fault. *Eng J* 25(1):43–52. <https://doi.org/10.4186/ej.2021.25.1.43>
- Regnier J, Cadet H, Bonilla LF, Bertrand E, Semblat JF (2013) Assessing nonlinear behavior of soils in seismic site response: statistical analysis on KiK-net strong-motion data. *Bull Seismol Soc Am* 103(3):1750–1770. <https://doi.org/10.1785/0120120240>
- Roten D, Fäh D, Bonilla LF, Alvarez-Rubio S, Weber TM, Laue J (2009) Estimation of non-linear site response in a deep Alpine valley. *Geophys J Int* 178(3):1597–1613. <https://doi.org/10.1111/j.1365-246X.2009.04246.x>
- Seyhan E (2014) Spreadsheet of NGA-West 2 calculations. Pacific Earthquake Engineering Research Centre (PEER). CA
- SNI 1726:2019 (2019) Seismic resistance planning procedures for building and non-building structures. National Standardization Agency: Indonesia
- SNI 1726:2019 (2019) Earthquake resistance planning procedures for building and non-building structures. National Standardization Agency, Jakarta, Indonesia
- Somantri AK, Mase LZ, Susanto A, Gunadi R, Febriansya A (2023) Analysis of ground response of bandung region subsoils due to predicted earthquake triggered by Lembang Fault, West Java Province, Indonesia. *Geotech Geol Eng* 41(2):1155–1181. <https://doi.org/10.1007/s10706-022-02328-x>
- Stone I, Wirth EA, Frankel AD (2022) Topographic response to simulated M_w 6.5–7.0 earthquakes on the seattle fault. *Bull Seismol Soci Am* 112(3):1436–1462. <https://doi.org/10.1785/0120210269>

- Supendi P, Nugraha AD, Puspito NT et al (2018) Identification of active faults in West Java, Indonesia, based on earthquake hypocenter determination, relocation, and focal mechanism analysis. *Geosci Lett* 5(1):1–10. <https://doi.org/10.1186/s40562-018-0130-y>
- Tanapalungkorn W, Mase LZ, Latcharote P, Likitlersuang S (2020) Verification of attenuation models based on strong ground motion data in Northern Thailand. *Soil Dyn Earthq Eng* 133:106145. <https://doi.org/10.1016/j.soildyn.2020.106145>
- Tjokrodinuljo K (2000) Earthquake engineering. Department of civil engineering, Gadjah Mada University, Yogyakarta, Indonesia
- Widiyantoro S, Supendi P, Ardianto A, Baskara AW, Bacon CA, Damanik R et al (2022) Implications for fault locking south of Jakarta from an investigation of seismic activity along the Baribis fault, northwestern Java, Indonesia. *Scient Rep* 12(1):1–10. <https://doi.org/10.1038/s41598-022-13896-6>
- Yoshida N (2015) Seismic ground response analysis. Springer, Dordrecht

Publisher's Note Springer Nature remains neutral with regard to jurisdictional claims in published maps and institutional affiliations.

Springer Nature or its licensor (e.g. a society or other partner) holds exclusive rights to this article under a publishing agreement with the author(s) or other rightsholder(s); author self-archiving of the accepted manuscript version of this article is solely governed by the terms of such publishing agreement and applicable law.